WEST Inc.
Environmental
& Statistical
Consultants

Icebreaker Wind Aerial Survey Waterbird Report:

October 16, 2017 – May 29, 2018
Cuyahoga County, Ohio

30 July 2018

Submitted to:

Icebreaker Windpower, Inc.
LEEDCo, 50 Public Square, Suite 200, Cleveland, Ohio 44113

Prepared by:
Jennifer H. Stucker, Jason D. Carlisle, Diem Pham, & Wallace P. Erickson

Western EcoSystems Technology, Inc. (WEST) provides environmental and statistical consulting services and contract research nationally and internationally to industry, government, and private organizations. We offer clients a unique combination of field ecology and statistics to help solve on-going and contemporary resource challenges. Through the use of state-of-the-art statistical principles in design, conduct, and analysis of ecological field studies, WEST specializes in common sense, defensible, and professional approach to the solution of natural resource problems.

Visit us at: www.west-inc.com

Preferred report citation:

Stucker, J. H., J. D. Carlisle, D. Pham, and W. P. Erickson. 2018. Icebreaker Wind Aerial Waterbird Survey Report: October 16, 2017 – May 29, 2018, Cuyahoga County, Ohio. Prepared for Icebreaker Windpower, Inc. Cleveland, Ohio. Prepared by Western EcoSystems Technology, Inc. (WEST), Golden Valley, Minnesota; Laramie, Wyoming; and Fort Collins, Colorado; Cheyenne, Wyoming. July 30, 2018.

EXECUTIVE SUMMARY

Icebreaker Windpower, Inc. has proposed to construct Icebreaker Wind, a 6-turbine offshore wind energy demonstration project in Lake Erie. This final report details the results from this pre-construction survey effort to meet the first monitoring objective, which was to identify the waterfowl and waterbird species, numbers, distribution, and use of survey area. The survey effort followed the agency approved *Aerial Waterfowl and Waterbird Study Plan*, included within the Icebreaker Windpower Monitoring Plan. The aerial survey study area extended more than five kilometers (km; three miles [mi]) in all directions from the originally proposed seven turbine sites, with the final survey area of 14,950 hectares (ha; 36,942 US acres [ac]) of US waters.

Surveys were conducted every two weeks from mid-October 2017 through May 2018 using a Cessna 185 with amphibious landing gear and three trained observers. The 17 surveys were conducted along seven 10-km (6-mi) fixed parallel transects spaced at 2.2km (1.4-mi) intervals within the survey area, and on variable path commuting transect while approaching and departing the survey area. Two additional surveys, following the same methods, were flown to assess changes in bird use during periods of ice formation in the survey area. Data collection for all flights followed a distance sampling method in combination with a double-observer approach to estimate the detectability of birds. Results were analyzed following a multiple-covariate distance sampling (MCDS) and mark-recapture distance sampling. The detectability estimates were incorporated with the observed counts using a Horvitz-Thompson-like estimator for MCDS to derive seasonal bird densities within the survey area. Confidence intervals (CI, 90%) were developed using bootstrapping (7,000 iterations) to resample observed data.

The aerial surveys documented 16 species, and one unique genus-level taxa, *Scaup* spp., for a total of 1,649 groups (i.e., a group includes one or more individuals) of birds that included 12,185 bird observations. Within the survey area, gull species constituted 71% of all documented birds, including herring gull (22%), ring-billed gull (12%), great black-backed gull (3%*),* and Bonaparte's gull (1%), with the remainder consisting of unidentified gulls (*Larus* spp). The remaining observations in the survey area included waterfowl (23%), mergansers (less than 4%), waterbirds (less than1%) loons (less than 0.5%). Outside the survey area, gulls (58%) composed the majority of observations, followed by mergansers (20%), waterfowl (18%), waterbirds (less than 5%), and loons (less than 0.1%). The largest of flocks were gulls, with up to 600 individuals, were seen outside the survey area.

Birds were observed either in the air flying or on the water surface, swimming, or standing on ice. When in the survey area, waterfowl and mergansers were seen flying low and fast above the water four times as often as on the water, with the strength of the relationship varying by season. In the survey area, gulls were twice as likely to be observed on the water as flying, an observation similar outside the survey area, but gulls were almost twice as abundant. Loons were five to 10 times more likely to be found on the water as flying, when observed. During the ice condition survey, fewer birds were observed in the survey area, but when they were present, the proportion of birds sitting or standing on ice or swimming was greater than the proportion observed flying.

Bird relative abundance in relation with distance to shore and water depth varied by season and species (gulls compared to all other species). Relative abundance for most birds was lower at the distances, relative to other depths. The highest relative abundance was generally at distances nearer shore for species other than gulls. The relative abundance of gulls was highest at near-shore distances for most, but not all, seasons and ice conditions. Under ice formation conditions, the birds were seen more often near shore, but in deeper water (10-14 meters [33-46 feet deep]).

Overall bird density within the survey area was 9.37 birds/km^2 (90% CI: 3.96 - 23.94), and varied by season, with greatest densities observed in winter. The largest portion of the density came from gulls, with 6.38 gulls/km^2 (90% CI: 2.21 - 19.67), with the next most abundant group, waterfowl, observed at 2.64 waterfowl/km^2 (90% CI 0.52 - 5.36). Merganser density varied by season, but averaged 0.26 merganser/km^2 (90% CI: 0.04 - 0.58). Bird density in the survey area was highest in the winter relative to other seasons. Survey results are consistent with relative abundance estimates from prior surveys by Norris and Lott for the Ohio Department of Natural Resources. Estimates of density at this location were lower than estimates of relative abundance from elsewhere in the Great Lakes.

STUDY PARTICIPANTS

Western EcoSystems Technology

Jennifer Stucker	Wildlife Biologist and Project Manager
Jason Carlisle	Statistician
Diem Pham	QAQC Statistician
Mandy Kauffman	Statistician
Carmen Boyd	Tracking and Data Manager
Kassidy Nordyke	Database Management
Ashleigh Boyd	Data Management
Jeff Fruhwirth	GIS Specialist
Katie Wynne	Technical Editing Coordinator
Andrea Palochak	Technical Editor
Wallace Erickson	Senior Reviewer
Dan Kramer	Crew Leader and Aerial Observer
Kristin Kovach	Aerial Observer
Michael Picciuto	Aerial Observer
John Schwartz	Aerial Observer

ACKNOWLEDGEMENTS

In addition to the formal study participants listed, we publicly thank:

Kristen Nasman for early advice on study design and analysis,

Trent McDonald for insights on distance-sampling,

Michael Kleinsasser, Ray Tupling, and Jaime Thompson for varied assistance with R programming and figures,

Cecily Foo for assistance in setting up materials for the field surveys, and

Derek DeRuiter and Northwoods Aviation, Inc.

TABLE OF CONTENTS

LIST OF TABLES

LIST OF FIGURES

LIST OF APPENDICES

INTRODUCTION

Icebreaker Windpower, Inc. (Icebreaker) has proposed to construct Icebreaker Wind, a 6-turbine offshore wind energy demonstration project (Project) in Lake Erie, approximately 13 - 16 kilometers (km; 8 - 10 miles [mi]) off the shore of Cleveland, Ohio.

This survey effort follows the approved *Aerial Waterfowl and Waterbird Study Plan,* in coordination with Ohio Department of Natural Resources and U. S. Fish and Wildlife Service, dated August 8, 2017, that was developed for inclusion in the Icebreaker Windpower Monitoring Plan and submitted to the Ohio Power Siting Board on August 18, 2017. The specific avian monitoring methods were designed to meet the two objectives identified in the Monitoring Plan to characterize:

1. Waterfowl and waterbird species, numbers, distribution, and use of survey area, and
2. Whether or not any waterfowl or waterbird species are displaced from the survey area due to the presence of wind turbines.

The first objective has been assessed, and the results are described in this report, which serves as a pre-construction assessment and can provide baseline data for analyses supporting the second objective in years one and four following construction of turbines, as set forth in the Monitoring Plan. This report details the results from this pre-construction survey effort conducted between October 16, 2017, and May 29, 2018, to meet the first objective, which was to identify the waterfowl and waterbird species, numbers, distribution, and use of survey area.

This final report has been prepared pursuant to the Memorandum of Understanding (MOU) between the IWP and the Ohio Department of Natural Resources (ODNR) dated July 12, 2017, which requires Icebreaker WIndpower to submit the final report 60 days following the conclusion of field efforts for the survey (see, MOU paragraph F, Exhibit B).

METHODS

Background

This aerial waterfowl and waterbird survey design incorporates recommendations by Gilbert et al. (2013) to the Great Lakes commission on survey and data collection design, with the goal of maximizing data quality. These recommendations are consistent with standardized design and procedure approaches in support of offshore aerial surveys in the northern hemisphere (Buckland et al. 2004, Camphuysen et al. 2004, Fox et al. 2006, and Bailey et al. 2014). Additional consideration in the design included ensuring that the surveyed area would be of adequate size to assess potential displacement of the most distance-sensitive species present in the Great Lakes, loons (*Gavia* spp.), which have demonstrated evidence of displacement in Europe to a distance of 2.0 km (>1.2 mi) from turbines (Petersen et al. 2006). It was under these conditions that the study was designed and conducted.

Study Area

The aerial survey study areaextends 5.0 km (3.1 mi) in all directions from the originally proposed seven turbine sites, and 5.4 km (3.4 mi) in the southeasterly direction; distance from proposed Turbine 6 to the northwestern survey boundary is 5.7 km (3.5 mi). The core survey area encompasses 14,950 hectares (ha; 36,942 US acres [ac]) of US waters within Lake Erie (Figure 1). Water depths within the survey area range from 15-20 meters (m; 49-66 feet [ft]), and the surrounding area includes depths ranging from 0-22 m (0-72 ft; Figure 2). Substrates within the survey area are primarily mud, with some limited areas of sand and clay. Substrates in the surrounding area are similar, with the addition of bedrock interspersed with clay and sand in the nearshore (Figure 3).

Survey Design

Data collection for all flights followed a distance sampling method in combination with a double-observer approach to estimate the detectability of birds. These integrated sampling approaches were used to minimize double counting, account for variability among the observers, and account for the expected decline in detections over increasing distances and viewing complexity. These methods, when combined, can improve the estimates of population abundance within the survey area, and thereby increasing the likelihood of detecting change attributable to displacement rather than variable survey skill. Details about the analytical approach are covered within the Statistical Analysis.

Aerial Line Transects

Data were collected using two different line transect types: 1) Project fixed, and 2) commuting. Specifics about each transect type are described below.

Project Fixed Transects

Within the Project survey area, fixed transects were oriented perpendicular to the proposed turbine string to support a gradient design, the preferred method for assessing point-source disturbance impacts (Ellis and Schneider 1997), including at offshore wind turbines (Bailey et al. 2014). In order to maximize the flight space between the proposed turbines, parallel transects were established 2.2 km (1.4 mi) apart, and perpendicular to the turbine string, resulting in seven 10.0-km (6.2-mi) transects that were flown during each survey (Figure 1). Transects were spaced at a distance greater than 2.0 km to minimize possibility of double counting between transects (Camphuysen et al. 2004). Observations from the seven fixed transects were used for all analyses, including abundance estimation within the survey area. Fixed transects were sampled during every survey.

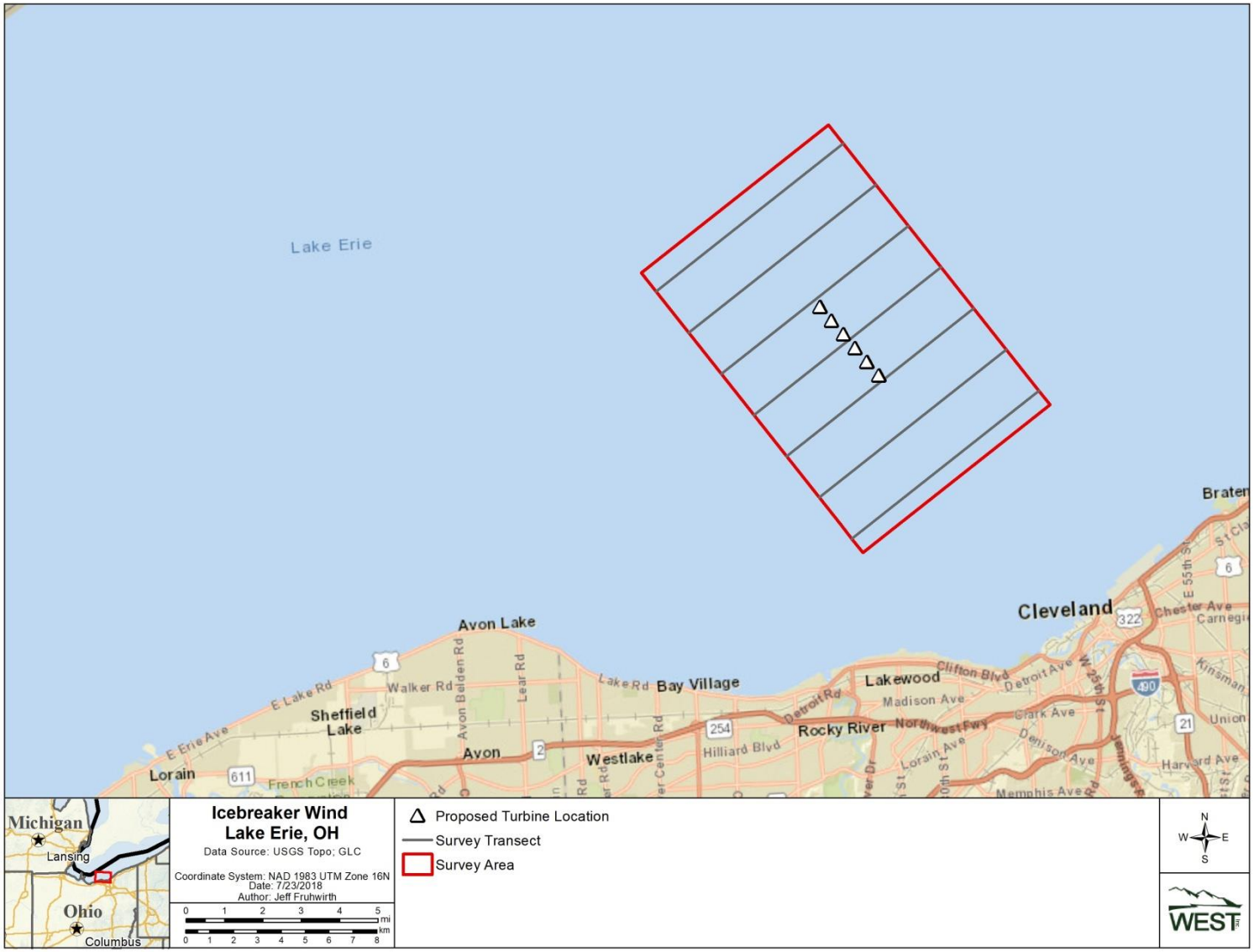

Figure 1. Location of the aerial survey area and survey transects for the Icebreaker Wind project.

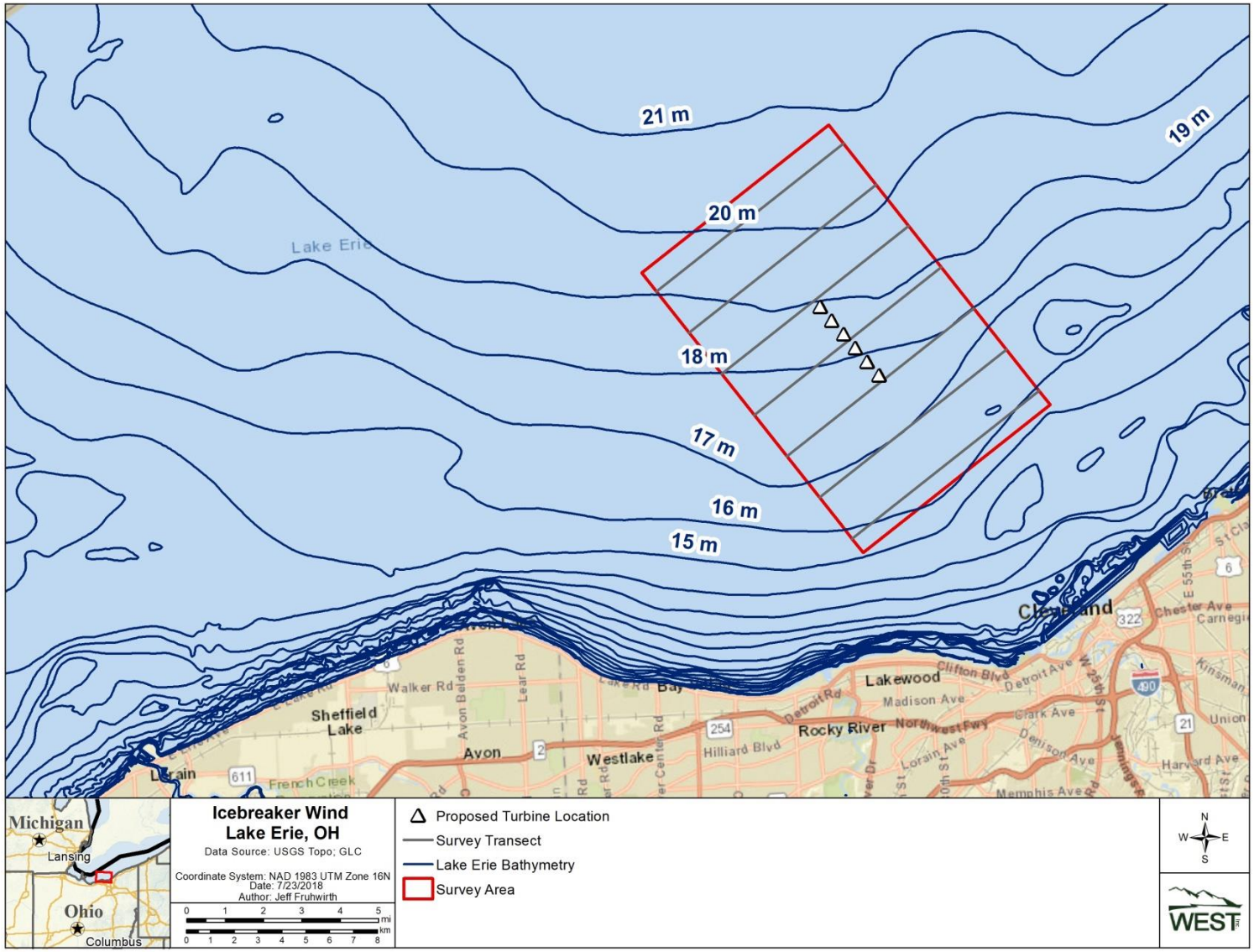

Figure 2. Bathymetry within the Icebreaker Wind project aerial survey area and surrounding areas.

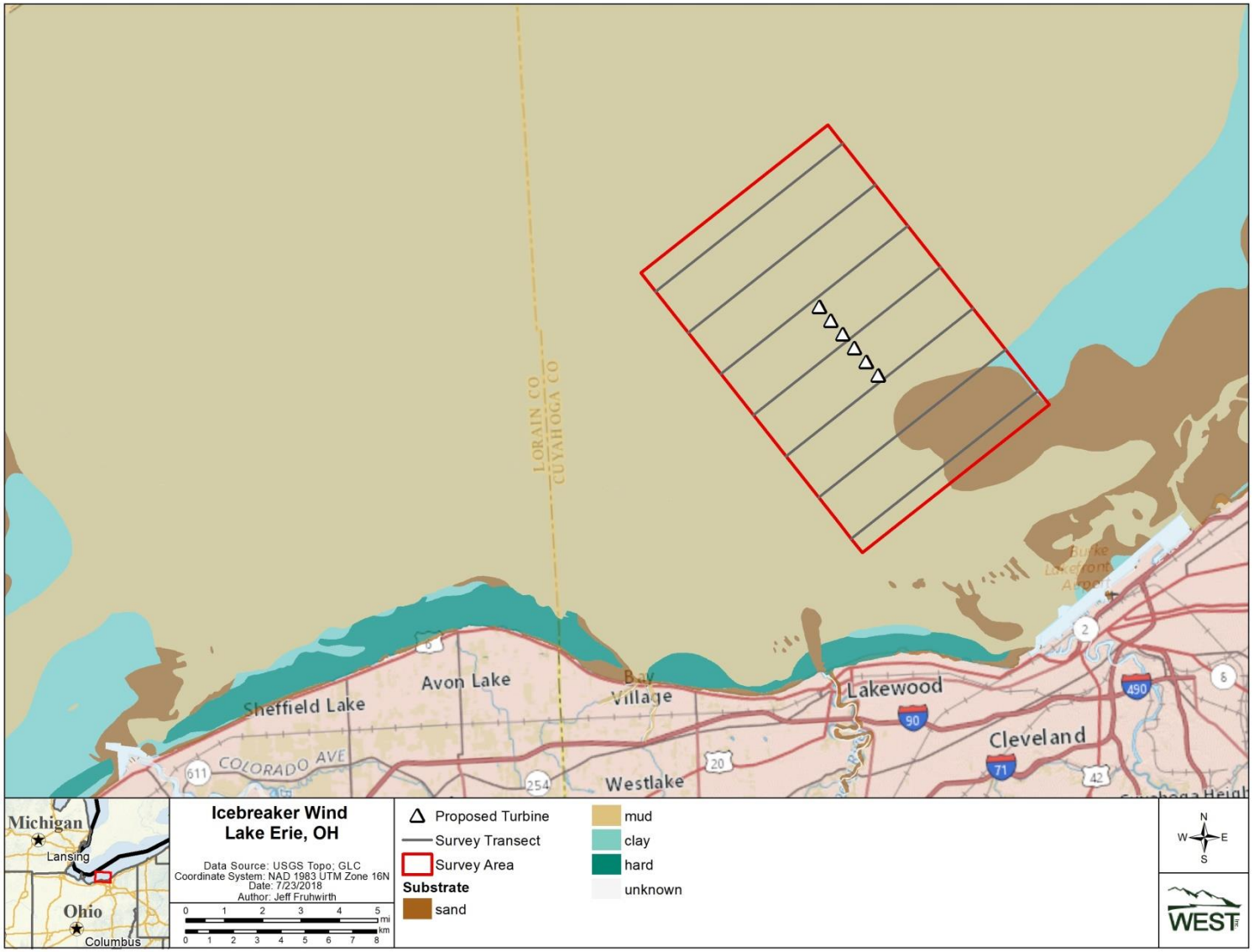

Figure 3. Substrate materials within the Icebreaker Wind project aerial survey area and surrounding areas..

Commuting Transects

After the first two surveys, two additional commuting flight path data collection "transects" were incorporated into each survey effort. The commuting transects provided an additional opportunity to document the distribution of species and raw counts of abundance outside the survey area, under varying observation conditions, particularly survey altitude and more variably sized groups of birds. The commuting flight paths were not fixed or determined beforehand; rather, they documented the direct non-looping paths selected by the pilot to approach and depart the survey area. Analysis of the commuting transect observation data was limited to aiding in development of the detection function, and assessing relationships between physical correlates (distance to shore and water depth). Data collected during the commuting transects should not be used to directly estimate density of birds following the formal sampling approach established for this survey due to the lack of any randomization in the selection of the location of the commuting transects.

Distance Estimation

Distance sampling requires accurate distance assessments during the observation process. Two objective approaches were used to estimate distance. First, distance bands (less than 60m; 60 – 100m; 100-150m; and additional 50m increments to greater than 500 meters), were established for all observations marks and were placed on the plane struts and on measuring rulers in the windows to constrain the subjective assessment; these tools were only valid at the survey elevation of approximately 76 m (249 ft)). Secondly, the vertical angle of depression from the observer to the object was recorded for each observation. This angle was measured automatically using Dioptra™, an Android-based application (app) for phones that takes a photo, and imposes measurements of direction, roll, and tilt on the image (Figure 4; Workshop512 2017). Using the X-coordinate, Y-coordinate, and Z-coordinate (altitude), location of the observer and the angle of depression, the bird group's location was estimated. Further details on this measurement approach are included in the Data Collection section below.

Figure 4. Example of Dioptra™ application image from the aerial survey on November 27, 2017, at the Icebreaker Wind survey area. This image documents the location of a loon swimming near Transect #7 in the survey area (yellow circle). The pictured angle of depression, -37.7 degrees (°) , is circled in red.

Double Observer

Conventional distance sampling methods assume certain detectability at some distance (traditionally at distance = 0; Buckland et al. 2001). Double-observer approaches use the statistical power of a mark-recapture model to relax this assumption by estimating the detectability at some distance, rather than assume certain detectability (Borchers et al. 2006, Burt et al. 2014).For this aerial survey, two observers were required on the right side of the plane to simultaneously and independently collect observations. These observations were later reconciled to determine what each observer saw or missed to correct for detection bias in the true number of birds. Complete independence between observers was maintained by visual separation through use of an opaque screen between the front and back observers, and all cabin-wide audio communication was halted during each transect survey with radio communication controlled by the pilot. Reconciliation of the double-observer sightings was completed as a separate process prior to analysis (see section below, Reconciliation of Double-Observer Data).

Temporal Considerations – Season, Survey Interval, and Diurnal Timing

The temporal sampling frame was identified in the Icebreaker Windpower MOU as mid-October to end of May to coincide with the greatest waterbird abundance and species occurrence in Lake Erie, based on prior pelagic survey efforts in the lake between 2009 and 2011 (Norris and Lott 2011). Within that period, we defined three seasons to assess seasonal changes in use: fall (October 16 – Nov 30), winter (December 1 – February 28), and spring (March 1 – May 29).

Survey timing was established on a systematic 2-week interval beginning October 15, 2017 through end of May 2018, per the MOU, for an anticipated 17 survey flights. Surveys were scheduled on the first day the weather was suitable for surveys and a survey crew was available. In addition to the 17 standard surveys, up to three supplementary ice condition surveys were planned when severe cold weather and lake ice forecasts predicted rapid and substantial ice formation within the survey area and surrounding area due to in-situ freezing, or wind and wave action moving ice sheets into the area.

Diurnal timing of surveys was scheduled across daylight hours as much as possible, with early-day (0500-1000 hours [H]), mid-day (1000-1400H) and later-day (1400-1900H) survey windows. Actual survey start times were modified to account for visible day length, and start times were shifted to avoid weather that would compromise favorable survey conditions (e.g., developing wind and waves, precipitation).

The survey start time, initial survey transect for the day, and travel direction along that transect were assigned randomly prior to the start of surveys in October.

Training Observers

Prior to the first survey, all observers attended two days of instruction that covered data collection methods to ensure consistency among observers, with instruction focusing on distance estimation, flock-size estimation, species identification. Instruction also included an aerial training flight over the study area and assurance that the electronic data collection process was feasible. Observers were encouraged and reminded to practice flock size estimation and species identification in the field, and using available aerial survey resources and training materials from the US Fish and Wildlife Services' Aerial Observer Training and Testing Resources program. Each observer was provided a copy of the *Aerial Observer's Guide to North American Waterfowl* (Bowman 2014) for the duration of the study.

Data Collection

Flights were completed using a Cessna 185 (high-wing, 4-seat airplane) with amphibious landing gear. High wing mounts ensured maximum visibility, and amphibious landing gear ensured ability to land on Lake Erie if necessary, but plane floats, while critical for survey safety, did block views under the plane. At flight height, the blocked are was 50m from the transect line. Each of the seven transects was sampled completely for each survey. Within the survey area, surveys were flown at a target of 76-m altitude above the lake surface, and at flight speeds of approximately 150 km per hour (kph; 93 mi per hour [mph]), or as close to the engine stall speed as possible. Outside the survey area, flight elevation and speed increased near land to

ensure safe operation. Flight tracks were documented with two identical Garmin eTrex ® 20x global positioning system (GPS) units with an accuracy of ± 3.7 m (12.0 ft), with track points collected every three seconds in first five of the 19 surveys, but every second for remainder of flights. Secondary tracks were collected on GPS-enabled Samsung S7 phones running the Locus Map Pro app (Asamm Software 2018) with an accuracy of less than five meters (16 ft).

Data collection during surveys was recorded digitally by each observer on Samsung S7 phones with an external microphone; observers had paper data sheets as backup during the flights. The data collection phones were set to GPS mode (no data signal) to ensure better location information, and touch sensitivity was maximized to ensure photo images were collected with no delay. In addition to the Locus Pro app, the Dioptra™ app (observation time, and angle depression to the bird), a voice recorder app was used to record continuously from just after takeoff through landing. At the start of each transect, the pilot would announce the transect start, which would prompt the observers to record transect-specific conditions (transect #, plane heading, visibility, and sea state). Bird observations were verbally recorded simultaneously with a Dioptra™ image taken perpendicular to the flight path. For each bird observation, the observer recorded the species, number of individuals, behavior, sex, age, the distance band, and additional features standard for a pelagic survey such as bird - object associations, pollution, percentage of ice at the observation site, and ice type following codes and descriptions. Gjerdrum et al.2012)

At the conclusion of the flight, all audio files were immediately transcribed by each observer, paper data sheets were visually inspected for completeness by another crew member, and data were entered into an electronic data entry form for upload into a relational database. If time and angle information was missing due to a missing Dioptra image, the time was estimated based on the time and duration of the audio recording. All datasheets were scanned, and copies of all electronic files (audio, GPS, photographs) were uploaded to a secure server for archiving. The original datasheets were shipped to WEST's office in Golden Valley, Minnesota, for ready access during quality assurance and quality control (QA/QC) processes, and to be archived.

Quality Assurance and Quality Control

QA/QC measures were implemented at all stages of the study, including in the field, during data entry and analysis, and report writing. Following field surveys, observers were responsible for inspecting data forms for completeness, accuracy, and legibility. A data technician then compared a sample of records from an electronic database to the raw data forms and corrected any errors. Irregular codes or data suspected as questionable were discussed with the observer or Project manager. Errors, omissions, or problems identified in later stages of analysis were traced back to the raw data forms and the electronic files, and appropriate changes in all steps were made.

Identifying Observer and Bird Locations

Consistent and unified observer locations were essential for accurately deriving the location of the bird with respect to the observer. Use of multiple GPS units simultaneously introduced user-specific locational error. Therefore, a single flight path GPS track for each flight was used to

assign accurate locations. Accurate locations were essential for reconciliation of observations, and to calculate the perpendicular distance (i.e., the distance between the bird group and the observer, perpendicular to the survey path), a value required as an input for distance-sampling analysis. The on-board GPS units collected *X*, *Y*, and *Z* point location typically every one to three seconds during flight, but the analysis required locations at 1-second intervals. We used a linear model to interpolate the location in each dimension for detections recorded in-between GPS track points to each second. The observation time, HH:MM:SS, was used to assign the location coordinates (*X*, *Y*, *Z)* from this GPS track location for each observation.

Second, we estimated the location of each bird group based on trigonometry of the right triangle formed with the vertices comprised of the observer (black circle in Figure 5), the bird (assumed to be on the lake surface, black star in Figure 5), and the water surface directly beneath the observer. Given the angle of depression recorded by the observer (θ in Figure 5) and the altitude of the observer above the lake level (length of side a in Figure 5), the analysis solved for the perpendicular distance between the observer and the bird group (length of side b in Figure 5) as

$$\tan(90-\theta) = \frac{opposite\ leg}{adjacent\ leg} = \frac{b}{a},$$

where $b = a \times \tan(90-\theta)$.

Third, we used the observer location, perpendicular distance, and plane heading, the direction of travel, to estimate the spatial location of the detected bird group. This spatial location was used for visualization and to attribute each bird group with spatial covariates associated with its location (e.g., distance from shore). To account for any discrepancy between the intended flight path and the actual flight path, we estimated the heading of the plane when the observation was made by calculating the heading between the on-board GPS waypoints two time-steps before and two time-steps after the time of detection. A time step was defined as the sequence of waypoints recorded by the on-board GPS.

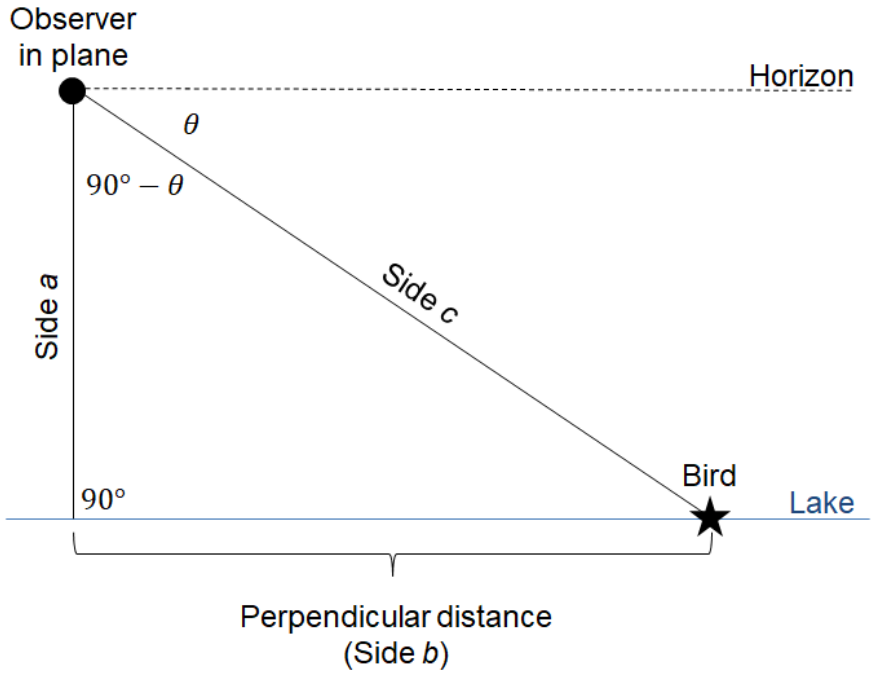

Figure 5. Diagram of right-triangle trigonometry used to estimate the perpendicular distance between the observer and the bird group for each group of birds detected.

Reconciliation of Double-Observer Data

At the conclusion of the QAQC process following assignment of locations to observers and birds, a systematic process was followed to reconcile each data observation between the front-right and back-right observers to identify when observations were the same, those that were only seen by the front seat observer, and those that were only seen by the back seat observer. Observations were matched using a series of criteria including: 1) time (less than seven seconds difference), 2) proximity between points in time and space, and 3) then the observer recorded information. Observer recorded information began with following: 1) observed species (or a similar species grouping), 2) survey flight path, 3) angle of observation, 4) distance band, 5) group size, 6) behavior, and 7) visual cues from plotting plane track and bird locations. In rare instances, additional decisions were made to combine observations within observers on a case-by-case basis for occasions when one observer documented a single flock and the other observer parsed the observations into two or more records; decisions to combine observations typically reduced the detail of the observation record for the analysis. Following this systematic process, the median difference in observation angle between observations considered a match was 9.5 degrees (80% of matched observations differing no more than 14 degrees between observers) and the median difference in number of individuals was zero (with 80% of matched observations differing not more than 1 individual between observers).

Statistical Analysis

Overview

Distance sampling is a common statistical method for estimating the abundance of animals while accounting for the imperfect ability of observers to detect all animals in field settings (Buckland et al. 2001). We used a combination of two model-based distance-sampling methods to estimate the detectability of waterbirds: multiple-covariate distance sampling (MCDS; Marques and Buckland 2003, Buckland et al. 2015) and mark-recapture distance sampling (MRDS; Borchers et al. 2006, Burt et al. 2014, Buckland et al. 2015). Given the estimates of detectability produced by these model-based methods, we used a simple design-based method to extrapolate from the observed count at sampled units to the average density within the survey area (Buckland et al. 2015). Basic distance-sampling methods include the assumption that all animals on the line are certain to be detected, but MRDS relaxes this assumption by estimating the detectability of animals on or near the transect (Buckland et al. 2001, Burt et al. 2014). And MCDS method relaxes the traditional assumption that detectability is constant across sites and individuals (Marques and Buckland 2003). Our approach to estimating density consisted of three steps:

1. Use distance-sampling data to estimate the probability of detecting each observed bird group, depending on the attributes of the bird group and the survey conditions;
2. Use mark-recapture data to properly scale the detection probabilities; and
3. Apply standard distance-sampling methods to inflate the number of waterbirds observed by the probability of detection and estimate waterbird density in the survey area by taxonomic group and season.

We conducted all analyses in Program R (R Core Team 2017), utilizing the Rdistance package (McDonald et al. 2018) for distance-sampling analyses.

Relative Abundance in Relation to Distance from Shore and Water Depth

We first conducted a preliminary spatial analysis to visualize the potential relationship between relative abundance (prior to correcting for detection probability) and two covariates that described the environmental conditions at and near the survey area: distance from shore and water depth. As appropriate, this preliminary analysis will be updated with a spatially explicit abundance maps corrected for detection probability.

We developed a gridded surface (raster) at 100-m (328-ft) spatial resolution (raster cells were a 100 x 100 m square) that covered the extent of all flight tracks, plus a 1.0-km (0.6-mi) buffer, and attributed each cell with the distance to the shoreline and water depth (National Geophysical Data Center 1999). We then calculated an index of relative abundance for each cell as the number of reconciled individuals observed across all surveys divided by the number of times that cell was surveyed (survey effort; a cell was considered surveyed if the centroid was within the 600-m [1,968-ft] wide surveyed area on either side of a flight track). The number of individuals observed was tabulated separately for gulls and other species. For example, if we

survey this area on 12 flights, but only saw birds 6, relative abundance for that cell would be 0.5. Both the numbers of individuals and effort were tabulated seasonally. We excluded 19 (of 1,649) bird groups that had due the raster grid, now had an estimated location on land. To visualize potential patterns, we averaged the index of relative abundance across surveyed cells within categories (e.g., cells zero to 1.0 km from shore) and plotted these averages by species group and season.

Estimating the Density of Birds in the Survey Area

Distance-sampling methods can be susceptible to instability when applied to small sample sizes of surveys or detected groups (Buckland et al. 2001, 2015). Although the primary objective was to estimate the density of birds in the survey area, we included data from the opportunistic surveys conducted while commuting to and from the survey area to improve model stability. These off-survey observations and detections collected during travel on the commuting transects were included in the analysis when modeling detection probabilities (Step 1 and Step 2), but excluded when estimating the density of birds in the survey area (Step 3).

Step 1 – Estimate Detection Probability with Multiple Covariate Distance Sampling (MCDS)

For line-transect surveys, the bulk of detections are typically nearest the observer (at small distances). However, in aerial surveys, a peak in the histogram of distances at some non-zero value of distance is common due to limited visibility directly under the aircraft and the relatively fast speed of travel (Buckland et al. 2001, 2015; Becker and Quang 2009; Nielson et al. 2014). One way to accommodate this peak at non-zero values of distance is to left-truncate the distance data (Buckland et al. 2001, 2015). Based on initial exploration of a Gaussian kernel smoother applied to our distance data (Sheather and Chris 1991, Wand and Jones 1995, Nielson et al. 2014), we identified an apparent peak in our distance distribution at 150 m (492 ft) for both gulls and other species (Figure 6). We chose to left-truncate any distances less than 150 m. Moreover, right-truncation where the probability of detection is approximately 0.15 is recommended to increase the robustness of distance-sampling analyses (Buckland et al. 2001, 2015). We chose to right-truncate any distances greater than 750 m (2,461 ft; Figure 6). Therefore, we analyzed data from a survey strip 600-m wide on both sides of the plane.

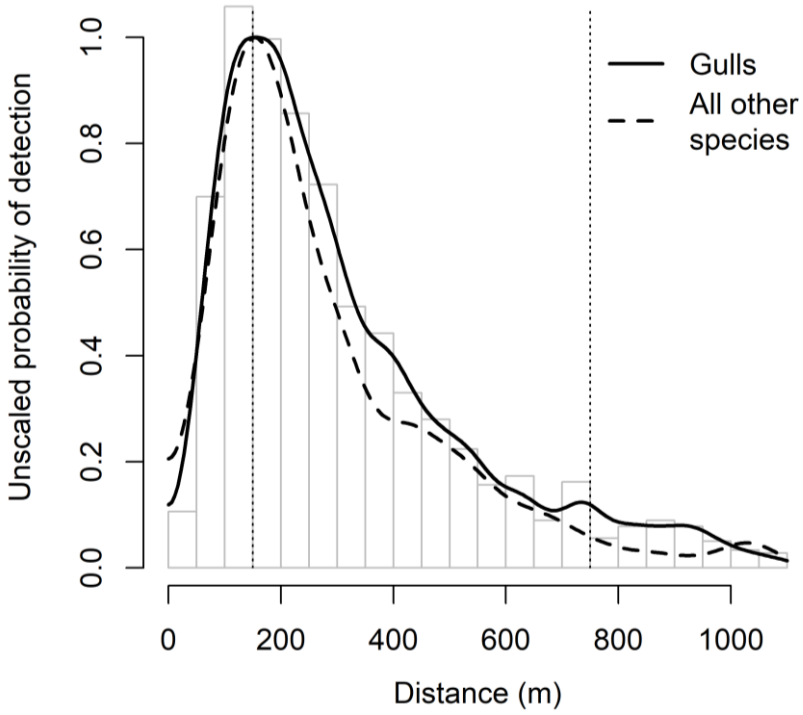

Figure 6. Estimated distances of bird detections from aerial avian surveys over Lake Erie, 2017 – 2018. A Gaussian kernel smoother applied separately for detections of gulls and all other species is shown over a histogram binned at 50-meter (m) intervals. Dotted lines show truncation distances used in analysis (left = 150 m, right = 750 m).

We identified five covariates expected to alter the detectability of birds: plane altitude, group size, taxonomic group, sea state, and survey type (Table 1). We formulated 32 competing models of detectability based on all possible additive combinations of these covariates and an intercept-only model that assumed detectability was constant. An initial comparison of detection functions fit using the half-normal, hazard-rate, and negative-exponential key functions revealed that the hazard-rate key function performed consistently better than the other two, so the models were limited to use the hazard-rate only. We defined the hazard-rate detection function as

$$g(x) = 1 - \exp\left(-\left(\frac{x}{\sigma_j}\right)^{-b}\right)$$

where x was the distance, b was the shape parameter, and σ was the scale parameter modeled as a function of covariates (Buckland et al. 2001, McDonald et al. 2018).

Table 1. Description of five covariates used to model the detectability of birds from aerial surveys at the Icebreaker Wind Project in Lake Erie, from October 16, 2017 – May 29, 2018.

Covariate	Type	Description
Plane altitude	Continuous	Altitude of the observer at the time of detection, recorded with on-board GPS; *log*-transformed to assist model convergence.
Group size	Continuous	Number of birds in the detected group; *log*-transformed to assist model convergence.
Species	Categorical	Two levels: gulls and other species.
Sea state	Categorical	Two levels: no waves (Beaufort sea states 0 – 1) and waves (Beaufort sea states ≥ 2).
Ice state	Categorical	Two levels: standard (regularly scheduled surveys with moderate to no ice cover) and ice (surveys conducted outside the regular schedule during peak ice cover).

We used an information-theoretic approach to rank the 32 competing models in the candidate set, based on the second-order variant of Akaike's Information Criterion (AICc; Burnham and Anderson 2002). Acknowledging that there is often uncertainty as to the best model in a candidate set, we opted to estimate the model-averaged unscaled detection probability ($\hat{\bar{P}}_j$) of each group j as the model-averaged prediction across all models in the candidate set (Burnham and Anderson 2002, Anderson 2008),

$$\hat{\bar{P}}_j = \sum_{i=1}^{R} w_i \hat{P}_{ij}$$

where R is the number of models, w_i is the AIC weight for model i (the weight of evidence in favor of model i; Burnham and Anderson 2002), and $\hat{P}_{ij}$ is the estimated unscaled detection probability for bird group j in model i. Model averaging produced model predictions (here, unscaled detection probabilities) that were not determined by any one model, but were instead calculated as weighted averages of these predicted values across multiple models (Burnham and Anderson 2002, Anderson 2008).

Step 2 – Scale Detection Probabilities Based on Mark-Recapture Distance Sampling (MRDS)

Conventional distance sampling assumes a probability of detection of 1.0 at distance = 0 (Buckland et al. 2001). Instead of assuming the probability of detection was known at some distance from the transect line, we used the mark-recapture trials generated by the two right-side observers to estimate the probability of detection at the distance from the transect line within the surveyed strip where the probability of detection was highest, assuming point independence at that distance (Borchers et al. 2006, Burt et al. 2014, Nielson et al. 2014). At the distance where detection rates were greatest, it was assumed that the MCDS detection function should equal the mark-recapture detection probability, so the MCDS detection function was scaled appropriately. We followed the general methodology for the point-independence MRDS variant described by Borchers et al. (2006) and detailed by Nielson et al. (2014). We excluded mark-recapture trials collected on Dec 27, 2017 from the mark-recapture datasets because the back-right observer was new and forgot to record some data during parts of this flight. As detailed in Nielson et al. (2014), we analyzed the mark-recapture data by estimating

the conditional probability of detection by the front-right observer (observer $k = 1$) given detection by the back-right observer (observer $k = 2$), ($p_{1|2}$), and the detection by the back-right observer given detection by the front-right observer ($p_{2|1}$) using logistic regression (Nelder and Wedderburn 1972).

We formulated 32 competing models of conditional detectability based on all possible additive combinations of five covariates (perpendicular distance and the covariates in the MCDS analysis excluding plane altitude; Table 1) and an intercept-only model that assumed conditional detectability was constant. An information-theoretic approach was used to rank the 32 competing models in the candidate set for each observer configuration ($p_{1|2}$ and $p_{2|1}$) based on AICc (Burnham and Anderson 2002). Acknowledging that there is often uncertainty as to the best model in a candidate set, we opted to estimate the model-averaged conditional detection probability ($\hat{\bar{p}}_{j,k|3-k}$) of each group j and observer k as the model-averaged prediction across all models in the candidate set (Burnham and Anderson 2002, Anderson 2008),

$$\hat{\bar{p}}_{j,k|3-k} = \sum_{i=1}^{R} w_i \, \hat{p}_{ij,k|3-k}$$

where R is the number of models, w_i is the AIC weight for model i (the weight of evidence in favor of model i; Burnham and Anderson 2002), and $\hat{p}_{j,k|3-k}$ is the estimated conditional detection probability for bird group j in model i for observer k. Model averaging produced model predictions (here, conditional detection probabilities) that were not determined by any one model, but were instead calculated as weighted averages of these predicted values across multiple models (Burnham and Anderson 2002, Anderson 2008).

Following the point-independence method (Borchers et al. 2006, Burt et al. 2014, Nielson et al. 2014) and assuming point independence at the left-truncation limit applied in the MCDS analysis (distance of $x = 150$ m from the aircraft), we estimated the probability of detection on the right side of the aircraft at distance x with covariate vector z_j by at least one observer as

$$p_{\bullet}(x, z_j) = p_{1|2}(x, z_j) + p_{2|1}(x, z_j) - p_{1|2}(x, z_j) p_{2|1}(x, z_j) .$$

Since mark-recapture trials were limited to the right side of the aircraft, it was assumed the probability of detection by the back-left observer was the same as $p_{2|1}(x, z_j)$ because both back-seat positions had the same visibility and we rotated observers among observation positions (Nielson et al. 2014). Last, we used these mark-recapture probabilities (specific to the side of the plane and the covariate vector z_j) to scale the previously unscaled estimates of detection probability ($\hat{\bar{P}}_j$) derived in the MCDS step of the analysis (Borchers et al. 2006, Nielson et al. 2014). For example, if the mark-recapture probability of detection of some bird group on the left side of the aircraft by the back-seat observer at $x = 150$ m from the aircraft was estimated as $p_{2|1}(150) = 0.6$, then the detection probability estimated for this bird group in the

MCDS step of the analysis would be scaled such that it equals 0.6 (Borchers et al. 2006, Nielson et al. 2014).

This scaled probability of detection was referred to as $\hat{\tilde{P}}_j^*$, and was calculated for groups detected on the right side of the plane as

$$\hat{\tilde{P}}_j^* = p_{\bullet}(x, z_j)\hat{\tilde{P}}_j ,$$

and for groups detected on the left side of the plane as

$$\hat{\tilde{P}}_j^* = p_{2|1}(x, z_j)\hat{\tilde{P}}_j .$$

Step 3 – Estimate Density by Taxonomic Group and Season

We calculated density (individuals per square km [km^2]) using the Horvitz-Thompson-like estimator for MCDS (Buckland et al. 2015) as

$$\hat{D} = \frac{A}{2wL}\sum_{j=1}^{n}\frac{s_j}{\hat{\tilde{P}}_j^*}$$

where $\hat{D}$ is density, A is the size of the study area (set to 1,000,000 to estimate density per km^2 based on transect lengths and strip widths measured in m), w is the strip half-width (600 m) and L is the total length (m) of surveyed strips. The number of detected groups is n, each group j with a group size (number of individuals) of s. $\hat{\tilde{P}}_j^*$ is the scaled detection probability for group j incorporating both the MCDS and MRDS components of detectability.

We estimated abundance separately by season (fall, winter-standard, winter-ice, spring, and overall [which excluded the Winter-Ice surveys conducted outside the regular survey schedule during peak ice cover]) and by taxonomic group (i.e., gulls, loons, mergansers, waterbirds, waterfowl, other, and all species combined) for a total of 35 estimates. We present estimates for season-species combinations only when detected groups were within the survey strips. We used a bootstrapping routine with 7,000 iterations to resample the 150 unique transect-visits (133 fixed transect visits [or surveys] within the survey area and 17 commuting transect visits) with replacement, re-ran the analysis steps 1 – 3 on each bootstrap realization of the data, and calculated a 90% confidence interval for each abundance estimate using the percentile method (Manly 1997).

RESULTS

Survey Effort

Seventeen standard surveys and two ice condition surveys were flown between October 16, 2017, and May 29, 2018. The ice condition flights were flown in January 2018 and February 2018, which were months with variable ice cover in the survey area. Surveys started as early as 0640H Eastern Standard Time (EST), with the latest start at 1400H EST, which during

December and January is late afternoon (Table 2). The first survey area transect and direction flown varied across the survey period (Table 2).

Table 2. Summary of completed aerial avian use surveys over Lake Erie for 2017 – 2018, at Icebreaker Wind, Cuyahoga County, Ohio including survey date and start time, starting transect, and initial heading.

Date	Survey Type and #	Transect Start Time (EST)	First Survey Area Transect	Initial Heading
October 16, 2017	Standard #1	10:00	4	NE
November 1, 2017	Standard #2	07:15	6	SW
November 13, 2017	Standard #3	13:40	5	SW
November 27, 2017	Standard #4	10:10	5	NE
December 11, 2017	Standard #5	08:10	3	NE
December 27, 2017	Standard #6	14:00	2	SW
January 4, 2018	Ice#1	10:20	1	NE
January 9, 2018	Standard #7	08:30	1	NE
January 25, 2018	Standard #8	14:00	5	SW
February 5, 2018	Standard #9	13:30	3	SW
February 17, 2018	Ice#2	08:15	7	NE
February 22, 2018	Standard #10	13:10	2	SW
March 5, 2018	Standard #11	11:00	4	SW
March 19, 2018	Standard #12	06:40	1	SW
April 2, 2018	Standard #13	12:40	3	SW
April 18, 2018	Standard #14	08:20	3	SW
April 30, 2018	Standard #15	06:50	7	NE
May 16, 2018	Standard #16	09:30	6	SW
May 29, 2018	Standard #17	13:25	7	NE

Observed Species

For the entire aerial survey, we documented 16 species, and one unique genus-level taxa, scaup unid (*Aythya marila + affinis)*, for a total of 1,649 groups (i.e., one or more individuals) of birds that included 12,185 individuals (Table 3; Appendix A). Most groups (67%) were of one bird, with 22% of groups including 2-10 birds, 8% with 22-50 birds, and 2% with a group size of 51-600 birds. Within the survey area, 14 species and one unique genus-level taxa, scaup unid (*Aythya marila + affinis)*, were observed. Observations within the survey area included 869 groups and 3,707 individuals. While overall seasonal abundance of all surveyed areas was greatest in winter, the patterns varied substantially among species and species-groups. For instance, Canada goose (*Branta canadensis*) was not observed in fall, relatively rarely in winter, and was most abundant in spring; but double-crested cormorant (*Phalacrocorax auritus*) was seen only in fall and spring. A single group of two passerines was observed in the fall, but no other species generally associated with terrestrial habitats were observed. No raptors or eagles were observed during surveys, either in the survey area, or over nearby waters.

Within the survey area, gull species constituted 71% of all documented birds. Gull species seen within the survey area included herring gull (*Larus argentatus;* 22%), ring-billed gull (*L. delawarensis;* 12%), great black-backed gull (*L. marinus;* 3%*),* and Bonaparte's gull

(*Chroicocephalus philadelphia;* 1%). About 34% percent of all birds recorded in the survey area were unidentified gull species. Following gulls, unidentified ducks (18%), followed by Canada goose (3.3%) were the most common species observed. All three merganser species were observed within the survey area, comprising 3.8% of all birds within the survey area. Merganser species observations included one observation of hooded merganser (*Lophodytes cucullatus*), two of common merganser (*Mergus merganser*), 31 of red-breasted mergansers (*Mergus serrator*), and 107 unidentified mergansers (3%). Common loon (*Gavia immer)* were observed 11 times, comprising less than 1% of birds observed in the survey area.

Within the commuting transects outside of the survey area, gulls composed 56% of all observations, including relatively large flocks of ring-billed gull (composing more than 3% of all observations), herring gull (more than 2%), great black-backed gull (1%), and Bonaparte's gull (less than 1%). Ten flocks of 100-600 individuals of unidentified gull species accounted for 67% of gulls observed on the commuting transects, some of the largest flocks seen. After gulls, unidentified ducks (13%), red-breasted mergansers (9.5%) and unidentified mergansers (10.4%) accounted for most remaining observations. Three species bserved during commuting flights in total represented between 1% - 5% of observations each, including: double-crested cormorants (4%); common goldeneye (*Bucephala clangula*; 4%), and Canada goose (2%). Fewer than 20 observations each of scoters (*Melanitta americana* or *Melanitta* spp.), loons, bufflehead (*B. albeola)*, scaup (*Aythya* spp.) or ring-necked ducks (*Aythya collaris*) were recorded. A single great-blue heron (*Ardea herodias*) was observed during a spring survey.

Table 3. Reconciled counts of bird groups (grp) and individuals (obs) by species observed during aerial survey flights between October 16, 2017 – May 29, 2018, within the Icebreaker Wind survey area (Survey) or along nearby commuting transects (Commute). Results are summarized by season (fall, winter, spring), and survey type (Standard or Ice).

	Season – Survey Type	*Fall – Standard*				*Winter – Standard*				*Winter – Ice*				*Spring – Standard*			
	Area	Survey		Commute		Survey		Commute		Survey		Commute		Survey		Commute	
	Flights	*n=4*		*n=2*		*n=6*		*n=6*		*n=2*		*n=2*		*n=7*		*n=7*	
Type	**Scientific Name**	**grp**	**obs**	**grp**	**obs**	**grp**	**obs**	**grp**	**obs**	**grp**	**obs**	**grp**	**obs**	**grp**	**obs**	**grp**	**obs**
Waterfowl		**14**	**19**	**8**	**24**	**27**	**618**	**50**	**1,029**	**9**	**59**	**12**	**335**	**12**	**131**	**19**	**292**
Canada goose	*Branta canadensis*	0	0	0	0	1	2	0	0	2	2	0	0	4	119	5	182
goose, unidentified	*Branta* spp.	0	0	0	0	0	0	0	0	0	0	1	2	0	0	0	0
ring-necked duck	*Aythya collaris*	0	0	1	9	0	0	0	0	0	0	0	0	0	0	0	0
scaup, unid	*Aythya* spp.	0	0	0	0	1	1	1	4	0	0	0	0	0	0	0	0
black scoter	*Melanitta americana*	1	1	1	8	0	0	2	7	0	0	0	0	0	0	0	0
scoter, unid	*Melanitta* spp.	2	2	0	0	0	0	0	0	0	0	0	0	1	1	0	0
long-tailed duck	*Clangula hyemalis*	0	0	0	0	1	2	0	0	0	0	0	0	0	0	0	0
Bufflehead	*Bucephala albeola*	1	1	0	0	0	0	1	20	0	0	0	0	0	0	0	0
common goldeneye	*Bucephala clangula*	0	0	0	0	2	3	14	235	3	8	2	19	1	1	4	56
duck, unidentified		10	15	6	7	22	610	32	763	4	49	9	314	6	10	10	54
Mergansers		**1**	**1**	**2**	**43**	**11**	**108**	**30**	**1,425**	**11**	**23**	**8**	**179**	**1**	**9**	**5**	**36**
hooded merganser	*Lophodytes cucullatus*	0	0	0	0	0	0	0	0	2	2	0	0	0	0	0	0
common merganser	*Mergus merganser*	0	0	0	0	1	1	0	0	0	0	0	0	0	0	0	0
red-breasted merganser	*Mergus serrator*	0	0	1	1	3	16	17	635	6	15	6	164	0	0	2	3
merganser, unidentified	*Mergus* spp.	1	1	1	42	7	91	13	790	3	6	2	15	1	9	3	33
Gulls		**153**	**227**	**36**	**42**	**313**	**1,934**	**337**	**3,772**	**112**	**326**	**75**	**316**	**176**	**194**	**169**	**592**
Bonaparte's gull	*Chroicocephalus philadelphia*	22	39	5	7	7	7	11	15	2	2	0	0	2	2	5	5
ring-billed gull	*Larus delawarensis*	40	46	8	9	102	218	104	170	45	85	22	25	85	93	55	68
herring gull	*Larus argentatus*	4	4	2	2	64	755	42	104	16	37	13	48	17	17	21	34
great black-backed gull	*Larus marinus*	0	0	0	0	23	64	27	53	20	35	12	27	0	0	5	5
gull, unidentified	*Larus* spp.	87	138	21	24	117	890	153	3430	29	167	28	216	72	82	83	480

Table 3. Reconciled counts of bird groups (grp) and individuals (obs) by species observed during aerial survey flights between October 16, 2017 – May 29, 2018, within the Icebreaker Wind survey area (Survey) or along nearby commuting transects (Commute). Results are summarized by season (fall, winter, spring), and survey type (Standard or Ice).

	Season – Survey Type	*Fall – Standard*				*Winter – Standard*				*Winter – Ice*				*Spring – Standard*			
	Area	Survey		Commute		Survey		Commute		Survey		Commute		Survey		Commute	
	Flights	*n=4*		*n=2*		*n=6*		*n=6*		*n=2*		*n=2*		*n=7*		*n=7*	
Type	**Scientific Name**	**grp**	**obs**	**grp**	**obs**	**grp**	**obs**	**grp**	**obs**	**grp**	**obs**	**grp**	**obs**	**grp**	**obs**	**grp**	**obs**
Loons		**11**	**12**	**2**	**2**	**0**	**0**	**1**	**1**	**0**	**0**	**0**	**0**	**0**	**0**	**1**	**1**
common loon	*Gavia immer*	10	11	2	2	0	0	1	1	0	0	0	0	0	0	1	1
loon, unidentified	*Gavia* spp.	1	1	0	0	0	0	0	0	0	0	0	0	0	0	0	0
Waterbirds		**3**	**15**	**1**	**1**	**1**	**2**	**3**	**12**	**0**	**0**	**0**	**0**	**3**	**6**	**12**	**347**
double-crested cormorant	*Phalacrocorax auritus*	3	15	1	1	1	2	3	12	0	0	0	0	3	6	11	346
great blue heron	*Ardea herodias*	0	0	0	0	0	0	0	0	0	0	0	0	0	0	1	1
Other		**1**	**1**	**5**	**6**	**7**	**19**	**2**	**2**	**1**	**1**	**0**	**0**	**2**	**2**	**2**	**21**
passerine, unid		0	0	1	2	0	0	0	0	0	0	0	0	0	0	0	0
medium bird, unid		0	0	0	0	4	12	0	0	0	0	0	0	1	1	1	20
large bird, unid		1	1	4	4	3	7	2	2	1	1	0	0	1	1	1	1
Total		**183**	**275**	**54**	**118**	**359**	**2,681**	**423**	**6,241**	**133**	**409**	**95**	**830**	**194**	**342**	**208**	**1,289**

Distribution of Observations

Mapped results of the reconciled observations for each of the 17 standard surveys and the two ice-condition surveys illustrate bird species, abundance, and survey track paths for each survey (Appendix A).

Bird Behavior and Location of Activity

Birds were observed either in the air flying or on the water surface, swimming, or standing on ice (Table 4). When in the survey area, waterfowl and mergansers were seen flying low and fast above the water four times as often as on the water, with the strength of the relationship varying by season. In the survey area, gulls were twice as likely to be observed on the water than flying, an observation similar outside the survey area, but gulls were almost twice as abundant. Loons were five to 10 times more likely to be found on the water as flying, when observed. During the ice condition survey, fewer birds were observed in the survey area, but when they were present, the proportion of birds sitting or standing on ice or swimming was greater than the proportion observed flying.

Table 4. Percent of reconciled counts of birds observed during aerial survey flights between October 16, 2017 – May 29, 2018, within the Icebreaker Wind survey area (Survey) or along nearby commuting transects (Commute). Results are summarized by season (fall, winter, spring), and survey type (Standard or Ice). Summarized for each taxonomic group (Type). Results are summarized by season (fall, winter, spring), and survey type (Standard or Ice), and the behavior/location when observed Flying (FL) or On Water/Ice (ON). Each row sums to 100% of observations by taxonomic group.

	Fall - Standard				Winter - Standard				Winter - Ice				Spring - Standard				Total %
	Survey *n=4*		Commute *n=2*		Survey *n=6*		Commute *n=6*		Survey *n=2*		Commute *n=2*		Survey *n=7*		Commute *n=7*		
Type	**FL%**	**ON%**	**FL%**	**ON%**	**FL%**	**ON%**	**FL%**	**ON%**	**FL%**	**ON%**	**FL%**	**ON%**	**FL%**	**ON%**	**FL%**	**ON%**	
Waterfowl	0	0	0	1	24	1	11	30	2	0	12	2	0	5	3	9	100
Mergansers	0	0	2	0	5	1	42	36	1	0	1	8	0	0	0	2	100
Gulls	3	1	0	0	6	20	16	35	2	3	1	3	2	1	2	6	100
Loons	6	69	0	13	0	0	0	6	0	0	0	0	0	0	0	6	100
Waterbirds	4	0	0	0	0	1	3	0	0	0	0	0	0	1	90	1	100
Others	0	2	4	8	23	13	4	0	0	2	0	0	0	4	2	38	100
Total %	2	1	1	0	9	13	18	33	2	2	3	4	1	2	5	6	100

Sums may not total values shown due to rounding.

Relative Abundance in Relation to Distance from Shore and Water Depth

The proposed turbine locations are approximately 12-15 km (seven to nine mi) from shore. The relative abundance of birds (accounting for survey effort but not corrected for imperfect detection) was generally low at these distances, relative to other distances. The highest relative abundance was generally at distances nearer shore for species other than gulls (Figure 7). The relative abundance of gulls was highest at near-shore distances for most, but not all, seasons and ice conditions (Figure 7). During peak ice conditions, relative abundances were highest approximately two to five km (one to three mi) from shore for both taxonomic groups (Figure 7).

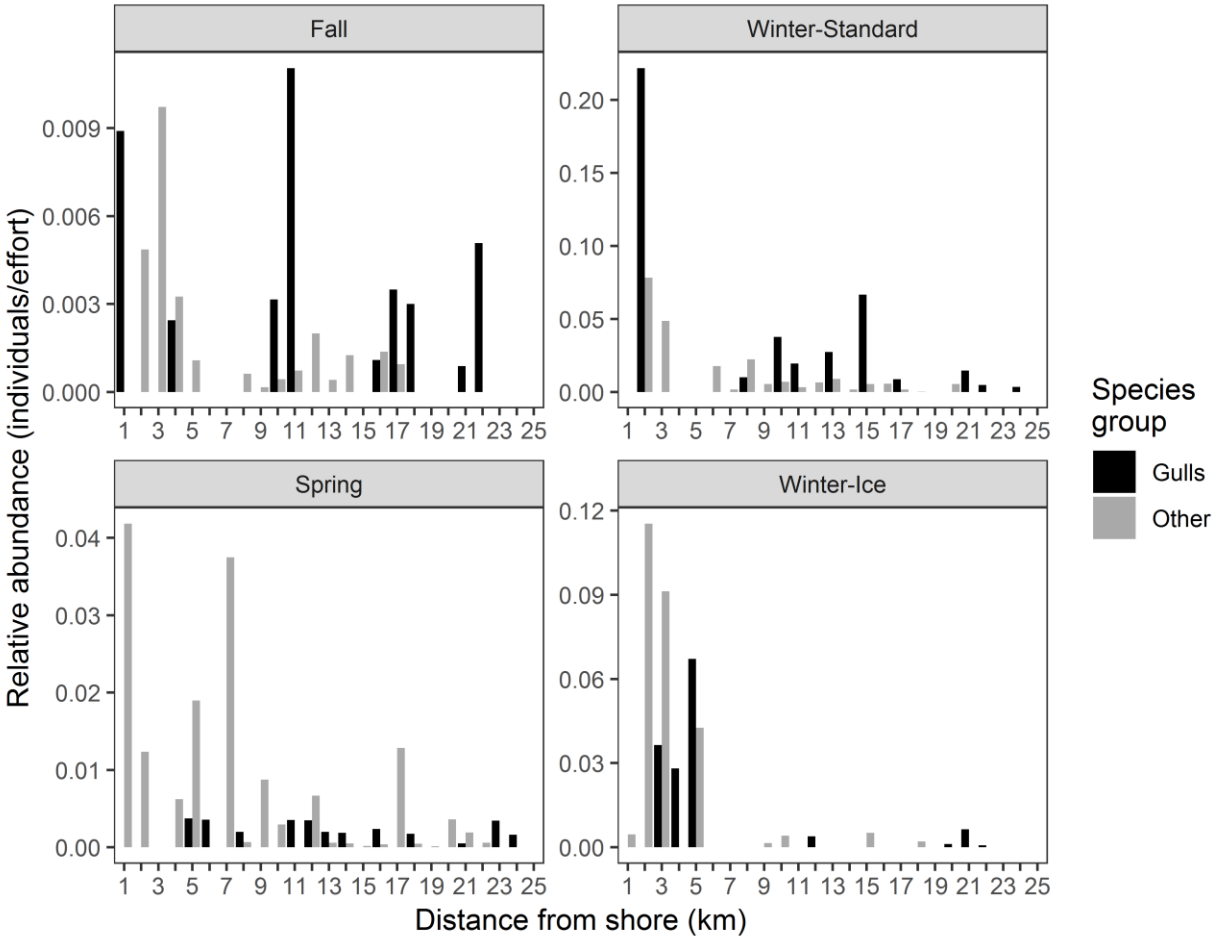

Figure 7. Mean relative abundance (birds/survey effort) for two taxonomic groups (gulls, all other species) in relation to distance from shore (kilometers [km]), by survey season (fall, winter, spring), and for the winter ice condition surveys. Distance from shore to the proposed turbine locations is approximately 12-15 km. Plots were based on reconciled observation data from the aerial avian surveys over Lake Erie 2017-2018, which have not been corrected for detectability.

The lake depth increased dramatically nearest the shore but was characterized by more gradual changes in depth elsewhere. Although distance from shore and water depth were correlated, this pattern in water depths created complexity in the relationship between distance from shore and water depth. The water depth at the proposed turbines was approximately 17 – 18 m (46 – 59 ft). The relative abundance of birds (accounting for survey effort but not corrected for

imperfect detection) was generally low in areas with these relatively shallower water depths. The highest relative abundances of gulls and other species were in areas where the lake was less than approximately eight to 10 m (26 to 33 ft) deep (Figure 8). However, in the winter surveys during peak ice conditions, non-gull species had highest relative abundance in areas where the lake was approximately 10-14 m deep (33 to 46 ft; Figure 8).

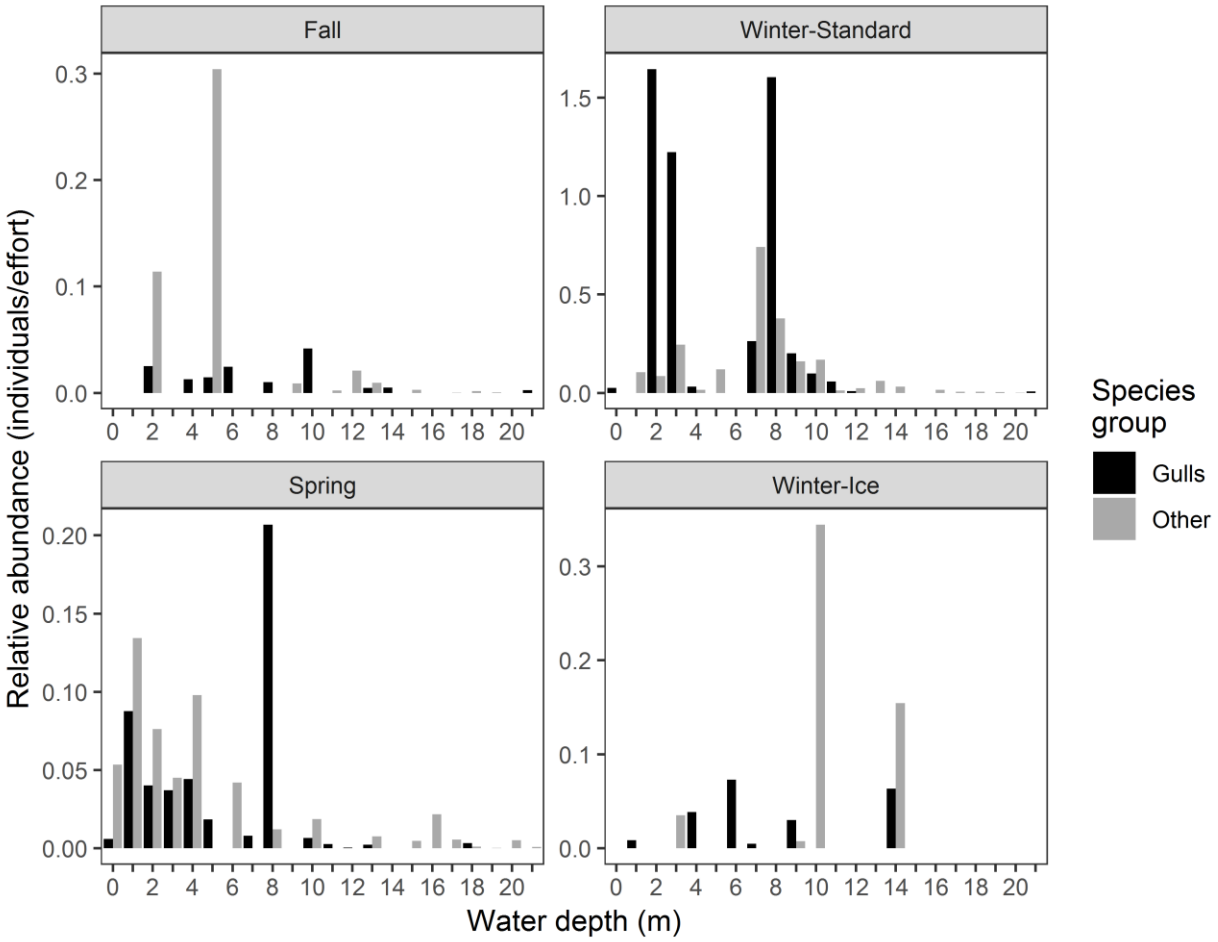

Figure 8. Mean relative abundance (birds/survey effort) for two taxonomic groups (gulls, all other species) in relation to water depth (meters [m]), by survey season (fall, winter, spring), and for the winter ice condition surveys. Water depths at the proposed turbine sites were 17–18 m. Plots were based on reconciled observation data from the aerial avian surveys over Lake Erie 2017-2018, which have not been corrected for detectability.

Density Estimates

Only 491 bird groups were observed within the survey strip (150-750 m [492-2,461 ft] perpendicular to the plane) during the 133 surveys in the Survey area. There was relatively little model-selection uncertainty in the MCDS portion of the analysis, with nearly all model weight distributed across the four highest-ranked models (Table 5). Detectability of birds varied by the survey conditions and attributes of the bird group. Detection probability was greatest during survey conditions with calmer sea state and less ice. Detection probability was greater at higher flight altitudes and when average group size was smaller. The mean of the unscaled detection

probabilities ($\hat{\bar{P}}_j$) for birds detected in the survey area was 0.38 (standard deviation [SD] = 0.11). There was relatively more model-selection uncertainty in the MRDS portion of the analysis. Depending on the observer configuration, nearly all model weight was distributed across the top eight to 12 highest-ranking models (Tables 6a and 6b). The mark-recapture probabilities varied by the survey conditions, attributes of the bird group, and observer position. Generally, mark-recapture probability was greatest at the near side of the surveyed strip, in survey conditions with calmer sea state and less ice. Generally smaller groups and species other than gulls had greater mark-recapture probability. On average, $p_{2|1}$ was greater than $p_{1|2}$. The mean mark-recapture probability ($p_{\bullet}$ for right-side observations and $p_{2|1}$ for left-side observations) for birds detected in the survey area was 0.73 (SD = 0.14). The mean of the scaled detection probabilities ($\hat{\bar{P}}_j^*$) for birds detected in the survey area was 0.28 (SD = 0.09); therefore, for each bird detected in the 600-m wide strip on either side of the plane (at 150-750 m perpendicular to the plane), there were 2.57 undetected birds on average.

We provide a heuristic example to assist in visualizing the detectability of birds documented within the survey strip (600 m wide) within the survey area. We show the median detection curve (assuming the average mark-recapture probability of 0.73) illustrating the effect of distance-from-the-plane on detectability. Because detectability was influenced by other variables (e.g., survey conditions and attributes of the bird group), we also show the 50% and 90% quantiles for group-specific detection curves (Figure 9).

Gulls were the most abundant species observed in the survey area, followed by waterfowl (Table 7, Figure 10). Both gulls and waterfowl were observed in all seasons. Loons, mergansers, waterbirds, and other birds (species for which identification was not possible in the field) were present in lesser abundances in the study area, and were not found in the survey strips within the survey area in all seasons (Table 3, Table 7, Figure 10). The density of each taxonomic group exhibited some variability by season, and overall, bird abundance was highest in the winter relative to other seasons.

Table 5. Model-selection results comparing candidate multiple-covariate distance sampling (MCDS) models to estimate the detectability of waterbirds during aerial surveys in Lake Erie, 2017 – 2018. The response variable in all models was the σ parameter of the hazard-rate detection function. Covariates are defined in Table 1. K is the number of parameters, corrected AICc is the second-order variant of Akaike's Information Criterion (AIC), ΔAICc is the difference between the model and the top-ranked model within the set, and *w* is the Akaike model weight. Models are ranked by AICc.

Model Covariates	K	AICc	ΔAICc	*w*
Plane altitude + Group size + Sea state + Ice state	6	12943.14	0.00	0.61
Plane altitude + Group size + Species + Sea state + Ice state	7	12945.16	2.01	0.22
Plane altitude + Sea state + Ice state	5	12946.80	3.66	0.10
Plane altitude + Species + Sea state + Ice state	6	12947.70	4.56	0.06
Plane altitude + Group size + Ice state	5	12954.65	11.51	0.00
Plane altitude + Group size + Sea state	5	12955.41	12.26	0.00
Plane altitude + Group size + Species + Ice state	6	12956.61	13.47	0.00
Plane altitude + Ice state	4	12956.75	13.61	0.00
Plane altitude + Group size + Species + Sea state	6	12957.40	14.26	0.00
Plane altitude + Species + Ice state	5	12958.33	15.19	0.00
Plane altitude + Sea state	4	12959.00	15.86	0.00
Plane altitude + Species + Sea state	5	12959.90	16.76	0.00
Group size + Sea state + Ice state	5	12975.71	32.56	0.00
Plane altitude + Group size	4	12976.35	33.21	0.00
Group size + Species + Sea state + Ice state	6	12977.63	34.49	0.00
Plane altitude	3	12978.18	35.04	0.00
Plane altitude + Group size + Species	5	12978.34	35.19	0.00
Plane altitude + Species	4	12979.85	36.70	0.00
Sea state + Ice state	4	12981.72	38.57	0.00
Species + Sea state + Ice state	5	12981.82	38.68	0.00
Group size + Sea state	4	12986.26	43.11	0.00
Group size + Species + Sea state	5	12988.15	45.01	0.00
Group size + Ice state	4	12990.81	47.67	0.00
Sea state	3	12992.50	49.36	0.00
Species + Sea state	4	12992.63	49.49	0.00
Group size + Species + Ice state	5	12992.83	49.69	0.00
Ice state	3	12994.99	51.84	0.00
Species + Ice state	4	12995.78	52.64	0.00
Group size	3	13012.48	69.34	0.00
Group size + Species	4	13014.50	71.36	0.00
1	2	13016.41	73.27	0.00
Species	3	13017.26	74.12	0.00

Table 6a. Model-selection results comparing candidate mark-recapture distance sampling (MRDS) models used to scale the distance-sampling-generated estimate of the detectability of birds during aerial surveys in Lake Erie, 2017 – 2018. The response variable in all models was the probability of detection by the front-right observer given detection by the back-right observer ($p_{1|2}$). Covariates are defined in Table 1. K is the number of parameters, AICc is the second-order variant of Akaike's Information Criterion, ΔAICc is the difference between the model and the top-ranked model in the observer-configuration set, and *w* is the Akaike model weight.

Model Covariates	K	AICc	ΔAICc	*w*
Distance + Group size + Sea state + Ice state	5	552.72	0.00	0.32
Distance + Group size + Species + Sea state + Ice state	6	553.38	0.65	0.23
Distance + Species + Sea state + Ice state	5	553.69	0.97	0.20
Distance + Sea state + Ice state	4	555.81	3.08	0.07
Group size + Sea state + Ice state	4	555.85	3.13	0.07
Group size + Species + Sea state + Ice state	5	556.66	3.93	0.05
Species + Sea state + Ice state	4	556.87	4.14	0.04
Sea state + Ice state	3	558.68	5.96	0.02
Distance + Group size + Species + Sea state	5	567.27	14.55	0.00
Distance + Species + Sea state	4	567.35	14.63	0.00
Distance + Group size + Sea state	4	567.40	14.68	0.00
Group size + Sea state	3	567.96	15.24	0.00
Group size + Species + Sea state	4	568.06	15.34	0.00
Species + Sea state	3	568.12	15.40	0.00
Distance + Sea state	3	570.79	18.07	0.00
Sea state	2	571.17	18.45	0.00
Distance + Species + Ice state	4	573.52	20.79	0.00
Distance + Group size + Species + Ice state	5	573.86	21.14	0.00
Distance + Group size + Ice state	4	574.63	21.91	0.00
Distance + Ice state	3	577.54	24.82	0.00
Distance + Species	3	580.26	27.54	0.00
Distance + Group size + Species	4	580.71	27.98	0.00
Species + Ice state	3	580.74	28.02	0.00
Group size + Species + Ice state	4	581.29	28.56	0.00
Group size + Ice state	3	581.84	29.12	0.00
Distance + Group size	3	582.07	29.35	0.00
Ice state	2	584.35	31.63	0.00
Species	2	584.37	31.65	0.00
Group size + Species	3	584.93	32.20	0.00
Distance	2	585.25	32.53	0.00
Group size	2	586.00	33.27	0.00
1	1	588.85	36.13	0.00

Table 6b Model-selection results comparing candidate mark-recapture distance sampling (MRDS) models used to scale the distance-sampling-generated estimate of the detectability of waterbirds during aerial surveys in Lake Erie, 2017 – 2018. The response variable in all models was the probability of detection by the back-right observer given detection by the front-right observer ($p_{2|1}$). Covariates are defined in Table 1. K is the number of parameters, AICc is the second-order variant of Akaike's Information Criterion, ΔAICc is the difference between the model and the top-ranked model in the observer-configuration set, and *w* is the Akaike model weight.

Model Covariates	K	AICc	ΔAICc	*w*
Distance + Group size + Species + Ice state	5	524.42	0.00	0.23
Distance + Group size + Ice state	4	524.55	0.13	0.21
Distance + Species + Ice state	4	525.92	1.51	0.11
Distance + Group size + Species + Sea state + Ice state	6	526.05	1.63	0.10
Distance + Group size + Sea state + Ice state	5	526.14	1.73	0.10
Group size + Ice state	3	526.80	2.39	0.07
Group size + Species + Ice state	4	527.20	2.78	0.06
Distance + Species + Sea state + Ice state	5	527.72	3.30	0.04
Group size + Sea state + Ice state	4	528.66	4.24	0.03
Species + Ice state	3	528.92	4.50	0.02
Group size + Species + Sea state + Ice state	5	529.09	4.67	0.02
Species + Sea state + Ice state	4	530.89	6.48	0.01
Distance + Ice state	3	532.25	7.84	0.00
Distance + Sea state + Ice state	4	534.12	9.70	0.00
Ice state	2	534.18	9.77	0.00
Sea state + Ice state	3	536.17	11.76	0.00
Distance + Group size + Sea state	4	536.69	12.27	0.00
Distance + Group size + Species + Sea state	5	537.53	13.11	0.00
Group size + Sea state	3	537.88	13.46	0.00
Distance + Group size	3	538.73	14.32	0.00
Group size	2	538.95	14.53	0.00
Group size + Species + Sea state	4	539.01	14.60	0.00
Distance + Group size + Species	4	539.68	15.26	0.00
Group size + Species	3	540.12	15.70	0.00
Distance + Species + Sea state	4	540.68	16.27	0.00
Species + Sea state	3	542.25	17.83	0.00
Distance + Species	3	542.44	18.03	0.00
Species	2	543.02	18.61	0.00
Distance + Sea state	3	545.59	21.18	0.00
Sea state	2	546.37	21.96	0.00
Distance	2	546.79	22.37	0.00
1	1	546.79	22.37	0.00

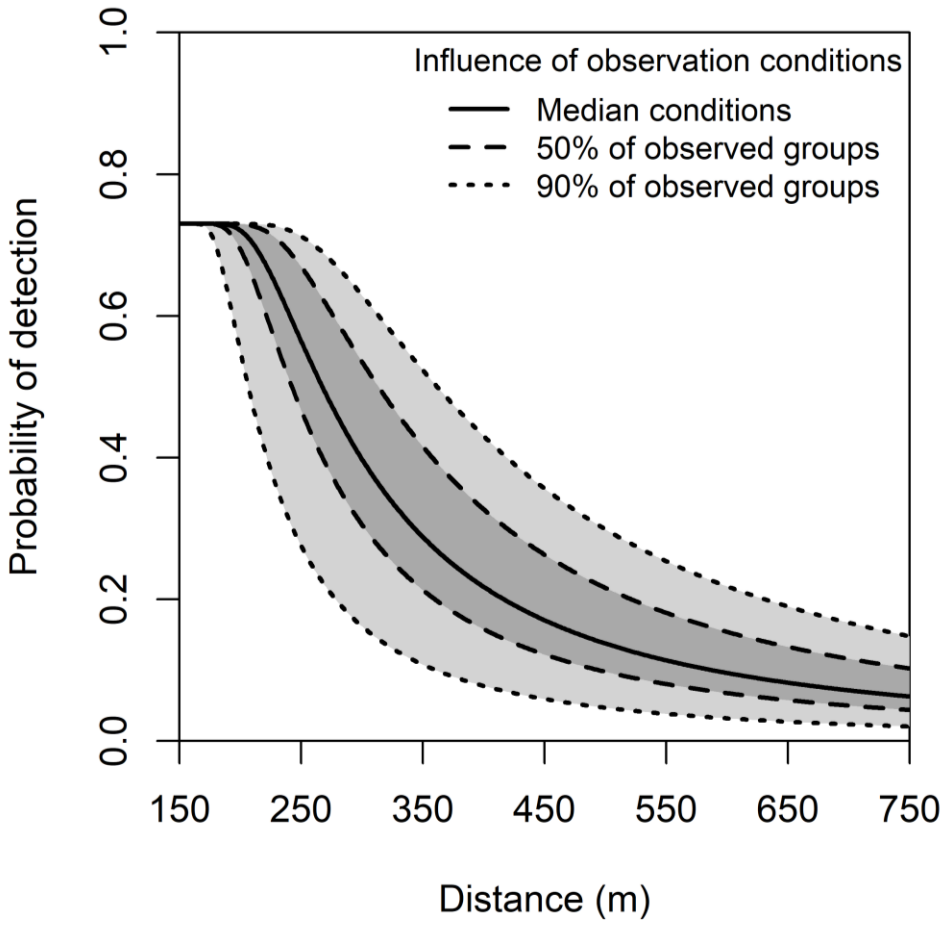

Figure 9. Example of scaled detection function of bird groups in the Icebreaker Wind survey area from aerial avian surveys in Lake Erie, 2017 – 2018. Predictions from the top-ranked Multiple Covariate Distance Sampling (MCDS) model (Akaike model weight = 0.61) are shown, scaled to the average Mark Recapture Distance Sampling (MRDS) probability of 0.73 assuming point independence at 150 m. Detectability varied based on attributes of the bird group and the surveying conditions, so we identified the median detection curve (across all groups detected in the surveyed strips in the survey area) and the regions that contain 50% and 90% of the detection curves.

Table 7. Estimated density (individuals/km^2) of bird taxonomic groups (Type) in the Icebreaker Wind survey area from aerial avian surveys in Lake Erie, 2017 – 2018. Intervals are bootstrap-generated 90% confidence intervals. No estimate or confidence interval is presented for seven taxonomic groups (Type) by season combinations for which no birds for a Type were detected in the survey strips in the survey area. The "Overall" season excluded the Winter-Ice surveys conducted outside the regular survey schedule during peak ice cover..

Types	Fall	Winter (Standard)	Winter (Ice)	Spring	Overall
Waterfowl	0.11 (0.01 - 0.23)	6.60 (0.44 - 14.14)	0.14 (0.00 - 0.35)	0.69(0.04 - 1.95)	**2.64 (0.52 - 5.36)**
Merganser	0.01 (0.00 - 0.03)	0.74 (0.10 - 1.62)	0.29 (0.00 - 0.98)	N/A	**0.26 (0.04 - 0.58)**
Gulls	1.57 (0.74 - 3.26)	16.34 (4.83 - 53.20)	3.48(1.81 - 5.80)	0.59 (0.45 - 0.73)	**6.38 (2.21 - 19.67)**
Loons	0.06 (0.01 - 0.14)	N/A	N/A	N/A	**0.01 (0.00 - 0.03)**
Waterbirds	0.05 (0.00 - 0.13)	N/A	N/A	0.04 (0.00 - 0.10)	**0.03 (0.01 - 0.06)**
Others	0.01 (0.00 - 0.03)	0.15(0.02 - 0.35)	0.06 (0.00 - 0.24)	N/A	**0.06 (0.01 - 0.13)**
All species	**1.80 (0.98 - 3.50)**	**23.83 (9.16 - 62.16)**	**3.96 (2.35 - 6.59)**	**1.31 (0.61 - 2.64)**	**9.37 (3.96 - 23.94**)

A. Single density range on y-axis for all species group plots.

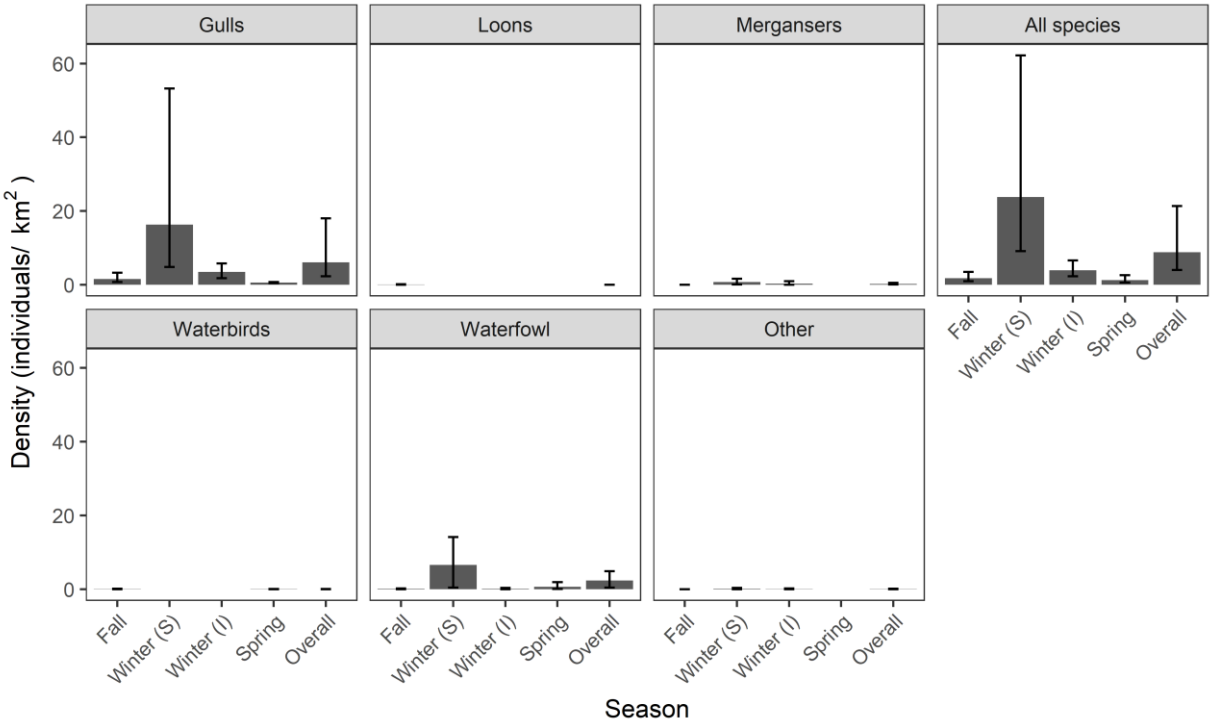

B. Varying density ranges on y axis for each species group plot

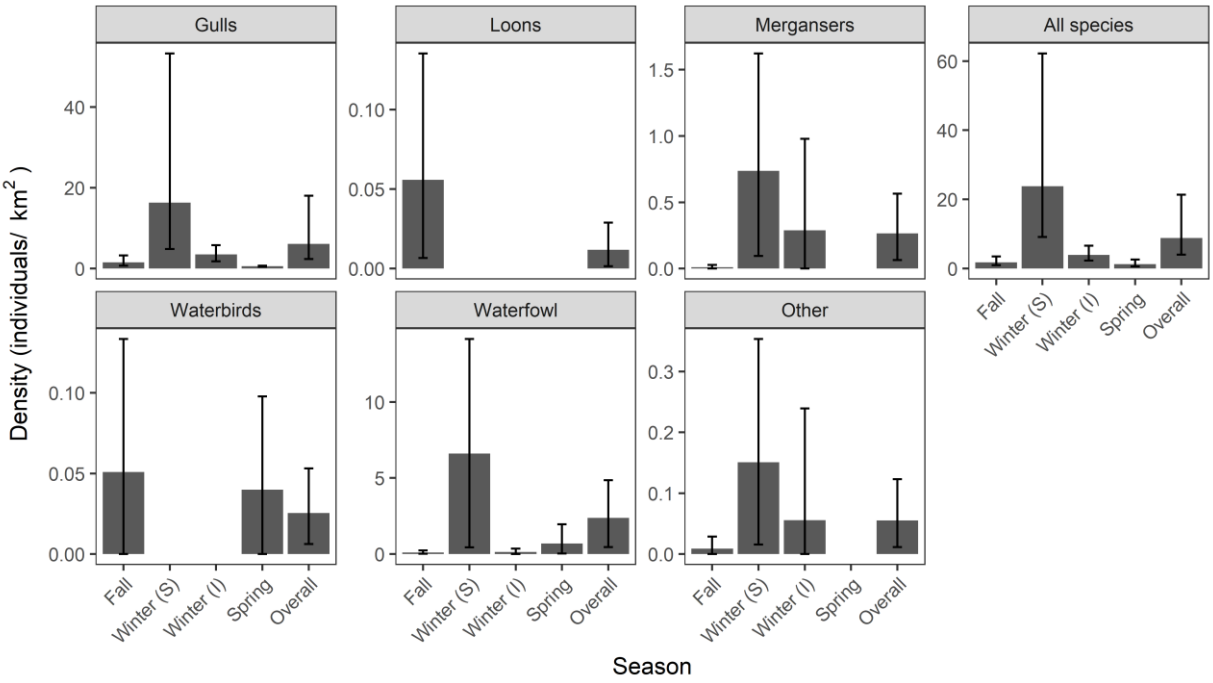

Figure 10. Estimated density estimates (individuals/km^2) for taxonomic groups by season in the Icebreaker Wind survey area from aerial bird surveys. Series A and B present equivalent information, but are portrayed with differing y-axes: a single density estimate range (A), and a varying density estimate (B). Error bars are bootstrap-generated 90% confidence intervals. No estimate or confidence interval was presented for a species-season combination that had no bird groups detected in the survey strips in the survey area. The "Overall" season excluded the Winter-Ice surveys conducted outside the regular survey schedule during peak ice cover.

DISCUSSION

The objective of this survey was to assess waterfowl and waterbird species, numbers, distribution, and avian use within a survey area surrounding the proposed Icebreaker Wind turbine locations. This survey marks the first double-observer study designed to estimate the density of birds while accounting for detectability in an offshore area of Lake Erie, and the first pre-construction site assessment for a proposed offshore wind facility in the Great Lakes. Prior aerial survey efforts in the Lake Erie offshore environment have focused on extensive spatial coverage of the Lake Erie shoreline (Norris and Lott 2011), providing substantial information about the diversity of species present, relative abundance, and temporal and spatial distributions during fall and spring seasons.

Although this study was conducted within a smaller geographic area relative to past aerial surveys of birds at the Great Lakes, our findings largely align with prior assessments for Lake Erie (Norris and Lott 2011; Lott et al. 2011), as well as additional work from Lake Huron and Lake Ontario. First, species diversity documented in this effort is comparable with prior surveys, given the extent of area surveyed and that our survey area was limited to open-water habitats with no marsh shoreline. All species observed in this study were reported previously, and in what appeared to be similar relative abundance (Norris and Lott 2011). Second, previous survey work indicated that most bird species tended to be distributed close to shore, with relative abundance declining in areas only a few kilometers offshore (Norris and Lott 2011; Stapanian and Waite 2003). On Lake Ontario, surveys by Long Point Waterfowl and Wetland Research Fund and Canadian Wildlife Service (Sea Duck Joint Venture 2007) found that observations of many waterfowl and waterbird species were most common when surveying transects 0.5 km parallel to shore. They concluded that >96% of their observations of bufflehead, common goldeneye, common merganser, and red-breasted merganser were located when flying the 0.5 km transect from shore, and these species were rarely observed when flying the 2 km transect from shoreline. Aerial surveys from Saginaw Bay similarly documented gulls as frequently observed at an undefined distance “far from shore” (Monfils and Gehring 2012). Results from this Icebreaker study are similar. During our winter surveys, particularly those when ice cover was highest, the near shore bird abundance appeared to increase shifted slightly offshore relative to areas more distant from shore; we suspect this shift was in response to the growth of the ice shelf at the shoreline. We assessed the relative abundance of birds in relation to water depth in a comparatively shallow area (<20 m depth) compared to the full range of depths surveyed by Lott et al (2011), but depth, unlike distance to shore, demonstrated some species specific variability, as described for individuals species in Lott et al (2011), an observation also by Stapanian and Waite (2003). Overall, the patterns we documented in the species, relative abundance, seasonal use, and distribution were largely consistent with prior assessments (Stapanian and Waite 2003, Norris and Lott 2011, Lott et al 2011).

This survey was initiated to provide a standardized and rigorous approach to estimate pre-construction bird densities in a manner that can be repeated after construction to assess potential attraction to or avoidance of turbine locations following construction. Pooling species and data collected during a standardized survey schedule, we estimated there are on-average

9.37 birds/km^2 (0.0937 birds/hectare [ha]) in the survey area, with 2.64 waterfowl/km^2 (0.0264 birds/ha). Work in Saginaw Bay by Monfils and Gehring (2011, 2012), and in the Eastern Staits of Mackainac and the eastern Upper Peninsula of Michigan (2013) provided a consistent and comparable survey and analysis approach although not double-observer corrected density estimates. For Saginaw Bay, density of waterfowl was a maximum density 0.56 waterfowl/ha in 2011 (Monfils and Gehring 2011) and a maximum density of 0.48 waterfowl/ha in 2012 (Monfils and Gehring 2012). Monfils and Gehring (2013) estimated a maximum density of 0.517 waterfowl/ha from northern Lake Huron to the east of the Straits of Mackinac, with a separate estimate for sea ducks of a maximum density of 0.087 sea ducks/ha. While seemingly comparable to this survey, it should be noted that the Monfils and Gehring (2011; 2012; 2013) estimates of relative abundance were not corrected for detectability and should therefore be considered minimum estimates (Caughley 1977), and that detectability can increase with density (Vrtiska and Powell 2011). While Saginaw Bay on Lake Huron may be ecologically more similar to the Sandusky Bay area of Lake Erie than the Icebreaker survey area, estimates of bird density are few for the Great Lakes. Therefore, although the Saginaw Bay estimates that do not account for detectability and are almost certainly an underestimate of the actual density, it is helpful to note that the Icebreaker survey area waterfowl density and overall bird density estimates are approximately 5% and 17%, respectively, of the 2010-2011 Saginaw bay estimates. Similarly, the estimated density of double-crested cormorants in the Icebreaker survey area is roughly 4% of those by Ridgeway (2010) for late-August (early migration) period out to 20 km from shore in northern Lake Huron, where Ridgeway (2010) estimated there were 1.21 cormorants per km^2 (95% CI= 0.78–1.70). At least for the period of the surveys we report here, the densities of waterfowl and waterbirds were less than other reported estimates from the Great Lakes. We acknowledge that there is a paucity of season and species-specific density estimates within the Great Lakes that account for detectability and would therefore facilitate a direct comparison to the estimates we report here.

REFERENCES

Anderson, D. R. 2008. Model Based Inference in the Life Sciences. Springer, New York, New York.

Asamm Software, s.r.o. 2018. Locus Map Pro - Outdoor GPS Navigation and Maps. Version 3.13.3. Information online: http://www.locusmap.eu/

Bailey, H., K. L. Brookes, and P. M. Thompson. 2014. Assessing Environmental Impacts of Offshore Wind Farms: Lessons Learned and Recommendations for the Future. Aquatic Biosystems 10: 8. doi: 10.1186/2046-9063-10-8.

Becker, E. F., and P. X. Quang. 2009. A gamma-shaped detection function for line-transect surveys with mark-recapture and covariate data. Journal of Agricultural, Biological, and Environmental Statistics 14: 207-223.

Borchers, D. L., J. L. Laake, C. Southwell, and C. G. M. Paxton. 2006. Accommodating Unmodeled Heterogeneity in Double-Observer Distance Sampling Surveys. Biometrics 62: 372-378.

Bowman, T. D. 2014. Aerial Observer's Guide to North American Waterfowl. USFWS publication FW6003. USFWS, Denver, Colorado.

Bradbury,G., Trinder M, Furness B, A. N. Banks, R. W. G. Caldow, and D. Hume. 2014. Mapping Seabird Sensitivity to Offshore Wind Farms. PLoS ONE 9(9): e106366. doi: 10.1371/journal.pone.0106366.

Buckland, S. T., D. R. Anderson, K. P. Burnham, J. L. Laake, D. L. Borchers, and L. Thomas. 2001. Introduction to Distance Sampling: Estimating Abundance of Biological Populations. Oxford University Press, Oxford.

Buckland, S. T., E. A. Rexstad, T. A. Marques, and C. S. Oedekoven. 2015. Distance Sampling: Methods and Applications. Springer, New York, New York.

Buckland, S. T., D. R. Anderson, K. P. Burnham, J. K. Laake, D. L. Borschers, L. Thomas, L. 2004. Advanced Distance Sampling. Oxford University Press, Oxford, United Kingdom.

Burnham, K. P. and D. R. Anderson. 2002. Model Selection and Multimodel Inference: A Practical Information-Theoretic Approach. Second Edition. Springer, New York, New York.

Burt, M. L., D. L. Borchers, K. J. Jenkins, and T. A. Marques. 2014. Using Mark-Recapture Distance Sampling Methods on Line Transect Surveys. Methods in Ecology and Evolution 5: 1180-1191.

Camphuysen, C. J., A. D. Fox, M. F. Leopold, and J. K. Petersen. 2004. Towards Standardised Seabirds at Sea Census Techniques in Connection with Environmental Impact Assessments for Offshore Wind Farms in the UK. A Comparison of Ship and Aerial Sampling Methods for Marine Birds and Their Applicability to Offshore Wind Farm Assessments. Report by Royal Netherlands Institute for Sea Research and the Danish National Environmental Research Institute to COWRIE BAM 02–2002. Crown Estate Commissioners, London, United Kingdom. Available online: https://tethys.pnnl.gov/sites/default/files/publications/Camphuysen-et-al-2004-COWRIE.pdf

Ellis, J. I. and D. C. Schneider. 1997. Evaluation of a Gradient Sampling Design for Environmental Impact Assessment. Environmental Monitoring and Assessment. 48: 157-172.

ESRI. 2017. World Imagery and Aerial Photos. ArcGIS Resource Center. ESRI, producers of ArcGIS software. Redlands, California. Information online: http://www.arcgis.com/home/webmap/viewer.html?useExisting=1

Fox, A. D., M. Desholm, J. Kahlert, T. K. Christensen, and I. K. Petersen. 2006. Information Needs to Support Environmental Impact Assessment of the Effects of European Marine Offshore Wind Farms on birds. Ibis 148(s1): 129-144. doi: 10.1111/j.1474-919X.2006.00510.x

Gilbert, A., W. Goodale, I. Stenhouse, and K. Williams. 2013. Preliminary Recommendations to Facilitate Data Collection During the Autumn 2013 Migration Season Great Lakes Aerial Surveys. A report to The Great Lakes Commission, Ann Arbor, Michigan.

Gjerdrum, C., D.A. Fifield, and S.I. Wilhelm. 2012. Eastern Canada Seabirds at Sea (ECSAS) Standardized Protocol for Pelagic Seabird Surveys from Moving and Stationary Platforms. Canadian Wildlife Service Technical Report Series No. 515. Atlantic Region. vi + 37 pp. Available online: http://publications.gc.ca/collections/collection_2012/ec/CW69-5-515-eng.pdf

Lott, K. D., M. Seymour, and B. Russell. 2011. Mapping Pelagic Bird Distribution and Abundance as a Decision-Making Tool for Offshore Wind Turbine Development and Conservation Planning. US Fish and Wildlife Service. Available online: https://www.fws.gov/midwest/fisheries/GLFWRA/30181-A-G011.pdf

Manly, B. F. J. 1997. Randomization, Bootstrap and Monte Carlo Methods in Biology. Second Edition. Chapman and Hall, London, United Kingdom.

Marques, F. F. C., and S. T. Buckland. 2003. Incorporating Covariates into Standard Line Transect Analyses. Biometrics 59: 924-935.

McDonald, T. L., R. M. Nielson, J. D. Carlisle, and A. McDonald. 2018. Rdistance: Analyses for distance-sampling and abundance estimation. R package version 2.1.1. Available online: https://github.com/tmcd82070/Rdistance

Nelder, J. A., and R. W. M. Wedderburn. 1972. Generalized Linear Models. Journal of the Royal Statistical Society 135: 370-384.

Nielson, R. M., L. McManus, T. Rintz, L. L. McDonald, R. K. Murphy, W. H. Howe, and R. E. Good. 2014. Monitoring Abundance of Golden Eagles in the Western United States. Journal of Wildlife Management 78: 721-730.

National Oceanic and Atmospheric Administration (NOAA). 2007. The Beaufort Wind Force Scale. NOAA/National Weather Service, National Centers for Environmental Prediction, Hydrometeorological Prediction Center, Camp Springs, Maryland.

National Geophysical Data Center, 1999. Bathymetry of Lake Erie and Lake Saint Clair. National Geophysical Data Center, NOAA. doi:10.7289/V5KS6PHK

Norris, J. and K. Lott. 2011. Investigating Annual Variability in Pelagic Bird Distributions and Abundance in Ohio's Boundaries of Lake Erie. Final report for funding award #NA10NOS4190182 from the National Oceanic and Atmospheric Administration, US Department of Commerce, through the Ohio Coastal Management Program, Ohio Department of Natural Resources, Office of Coastal Management. Available online: https://wildlife.ohiodnr.gov/portals/wildlife/pdfs/species%20and%20habitats/pelagic2011report.pdf

North American Datum (NAD). 1983. NAD83 Geodetic Datum.

Petersen, I. B., T. K. Christensen, J. Kahlert, M. Desholm, and A. D. Fox. 2006. Final Results of Bird Studies at the Offshore Wind Farms at Nysted and Horns Rev, Denmark. National Environmental Research Institute, Ministry of the Environment, Denmark. 161 pp. Available online: http://www.folkecenter.eu/FC_old/www.folkecenter.dk/mediafiles/folkecenter/pdf/Final_results_of_bird_studies_at_the_offshore_wind_farms_at_Nysted_and_Horns_Rev_Denmark.pdf

R Core Team. 2017. R: A Language and Environment for Statistical Computing. R Foundation for Statistical Computing, Vienna, Austria.

Sheather, S. J., and J. Chris. 1991. A Reliable Data-Based Bandwidth Selection Method for Kernel Density Estimation. Journal of the Royal Statistical Society: Series B (Statistical Methodology) 53: 683-690.

US Fish and Wildlife Service (USFWS). 2018. Aerial Observer Training and Testing Resources. Information online: https://www.fws.gov/waterfowlsurveys/welcome.jsp?menu=home

US Geological Survey (USGS). 2016. Version 10.22. ArcGIS Rest Services Directory. Streaming data. The National Map, USGS. Last updated September 2016. Information online: https://basemap.nationalmap.gov/arcgis/rest/services

Wand, M. P., and M. C. Jones. 1995. Kernel Smoothing. Chapman & Hall/CRC, Boca Raton, Florida.

Workshop512. 2017. Dioptra ™ - A Camera Tool. Version 1.0.10. Information online: https://play.google.com/store/apps/details?id=com.glidelinesystems.dioptra

Caughley, G. 1977. Analysis of vertebrate populations. John Wiley & Sons, Chichester, West Sussex, UK.

Monfils, M. J., and J. L. Gehring. 2011. Identifying migrant waterfowl and waterbird stopovers to inform wind energy development siting within Saginaw Bay – year 1 report. Michigan Natural Features Inventory, Report Number 2011-16, Lansing, MI.

Monfils, M. J., and J. L. Gehring. 2012. Identifying migrant waterfowl and waterbird stopovers to inform wind energy development siting within Saginaw Bay. Michigan Natural Features Inventory, Report Number 2012-19, Lansing, MI.

Monfils, M. J., and J. L. Gehring. 2013. Identifying migrant waterfowl and waterbird stopovers to inform offshore wind energy development in the eastern Upper Peninsula. Michigan Natural Features Inventory, Report Number 2013-14, Lansing, MI.

Ridgway, M. S. 2010. Line Transect Distance Sampling in Aerial Surveys for Double-Crested Cormorants in Coastal Regions of Lake Huron. Journal of Great Lakes Research 36:403-410

Sea Duck Joint Venture. 2007. Recommendations for monitoring distribution, abundance, and trends for North American Sea Ducks. Report produced by the Sea Duck Joint Venture. https://seaduckjv.org/pdf/studies/pr95.pdf

Stapanian, M. A. and T. A. Waite. 2003. Species density of waterbirds in offshore habitats in western Lake Erie. Journal of Field Ornithology 74:381-391.

Vrtiska, M. P., and L. A. Powell. 2011. Estimates of Duck Breeding Populations in the Nebraska Sandhills Using Double Observer Methodology. Waterbirds 34:96–101.

Appendix A
Location of the Aerial Survey Area, 750-Meter Buffer Survey Track, and Number of Birds Observed from October 16 2017 – May 29, 2018, at the Icebreaker Wind Survey Area

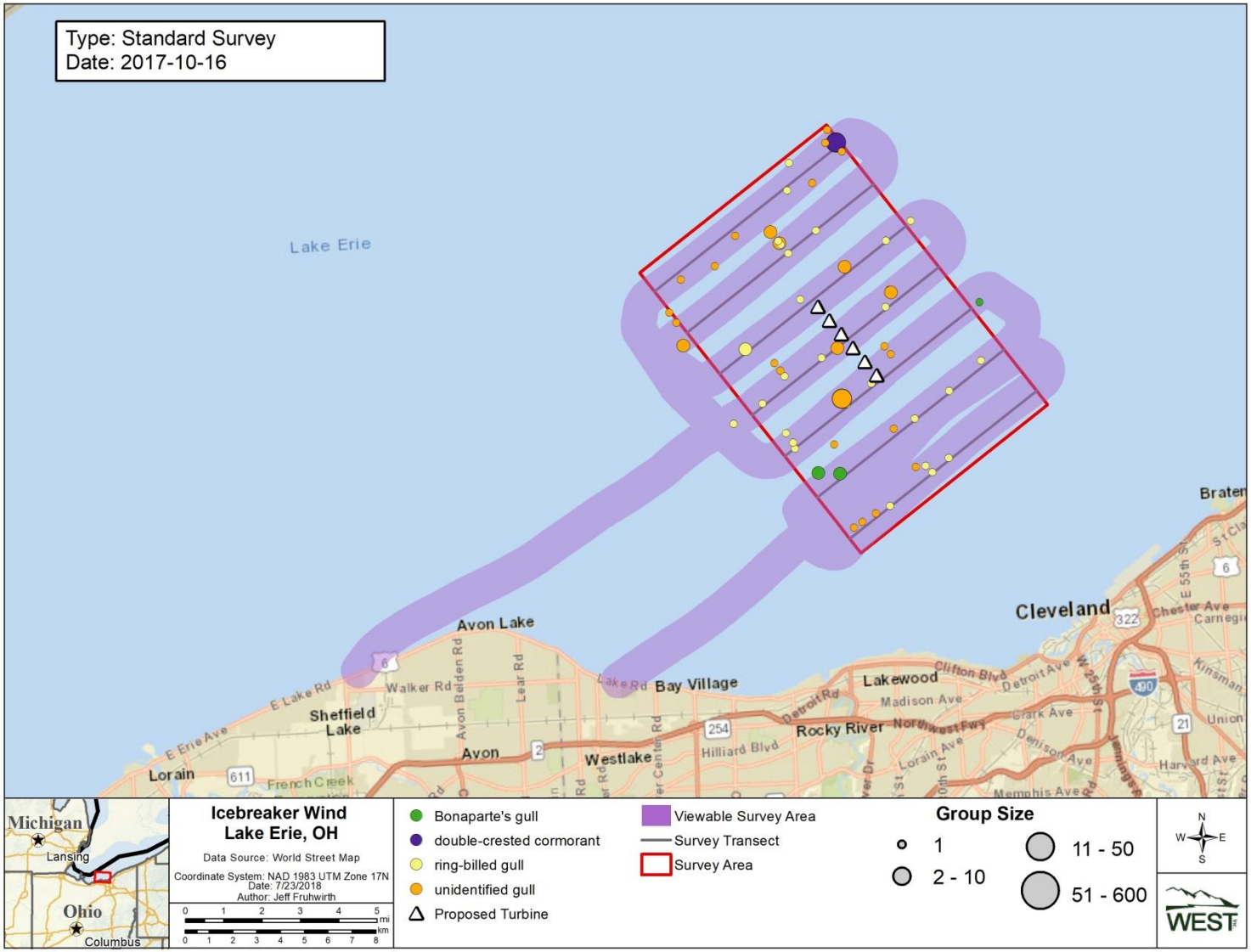

Appendix A-1. Location of the aerial survey area (red), 750-meter buffer survey track (purple), and number of birds (various colors; size of symbol indicates relative abundance) observed on October 16, 2017, for the Icebreaker Wind project. Bird counts and locations based on reconciled observations.

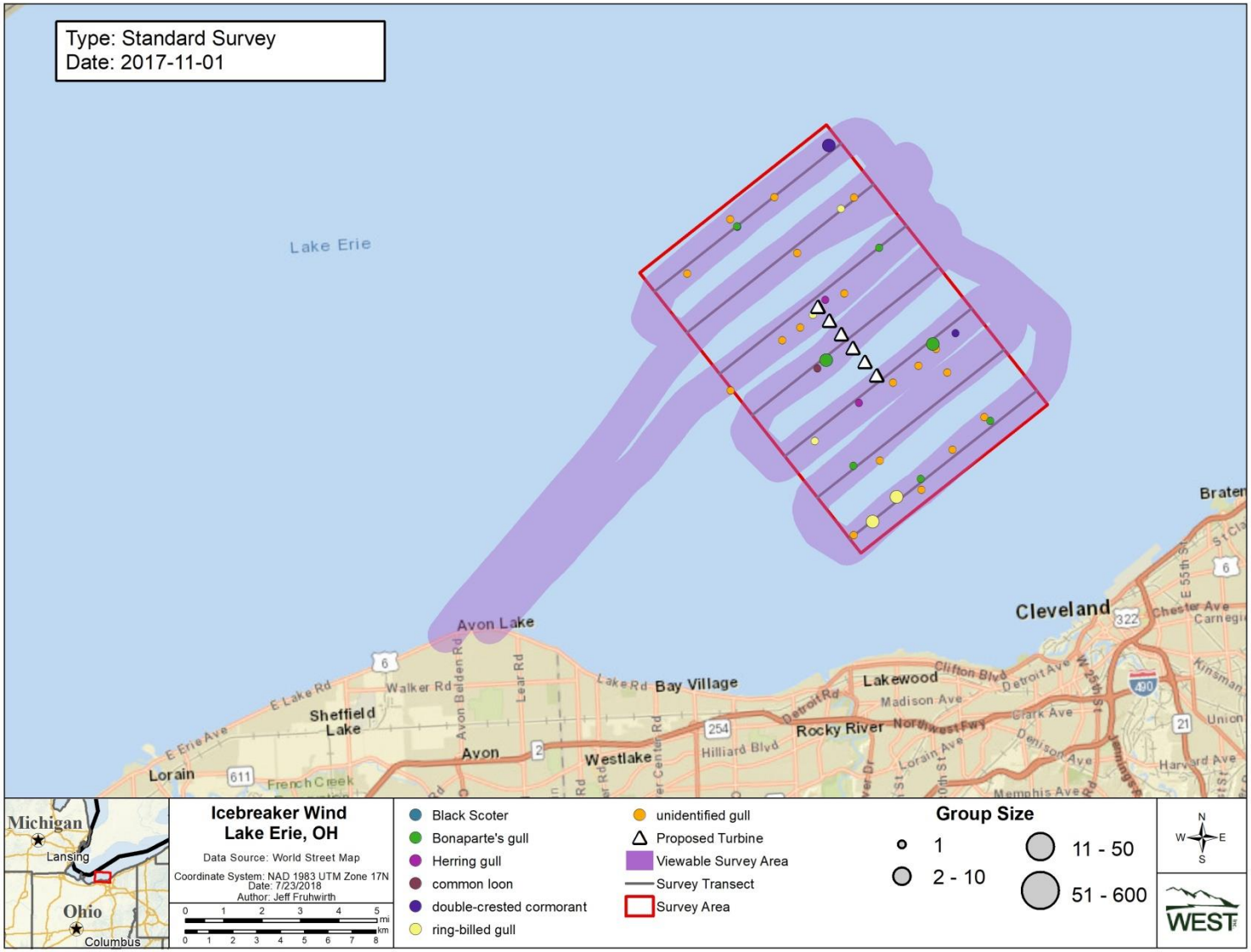

Appendix A-2. Location of the aerial survey area (red), 750-meter buffer survey track (purple), and number of birds (various colors; size of symbol indicates relative abundance) observed on November 1, 2017, for the Icebreaker Wind project. Bird counts and locations based on reconciled observation.

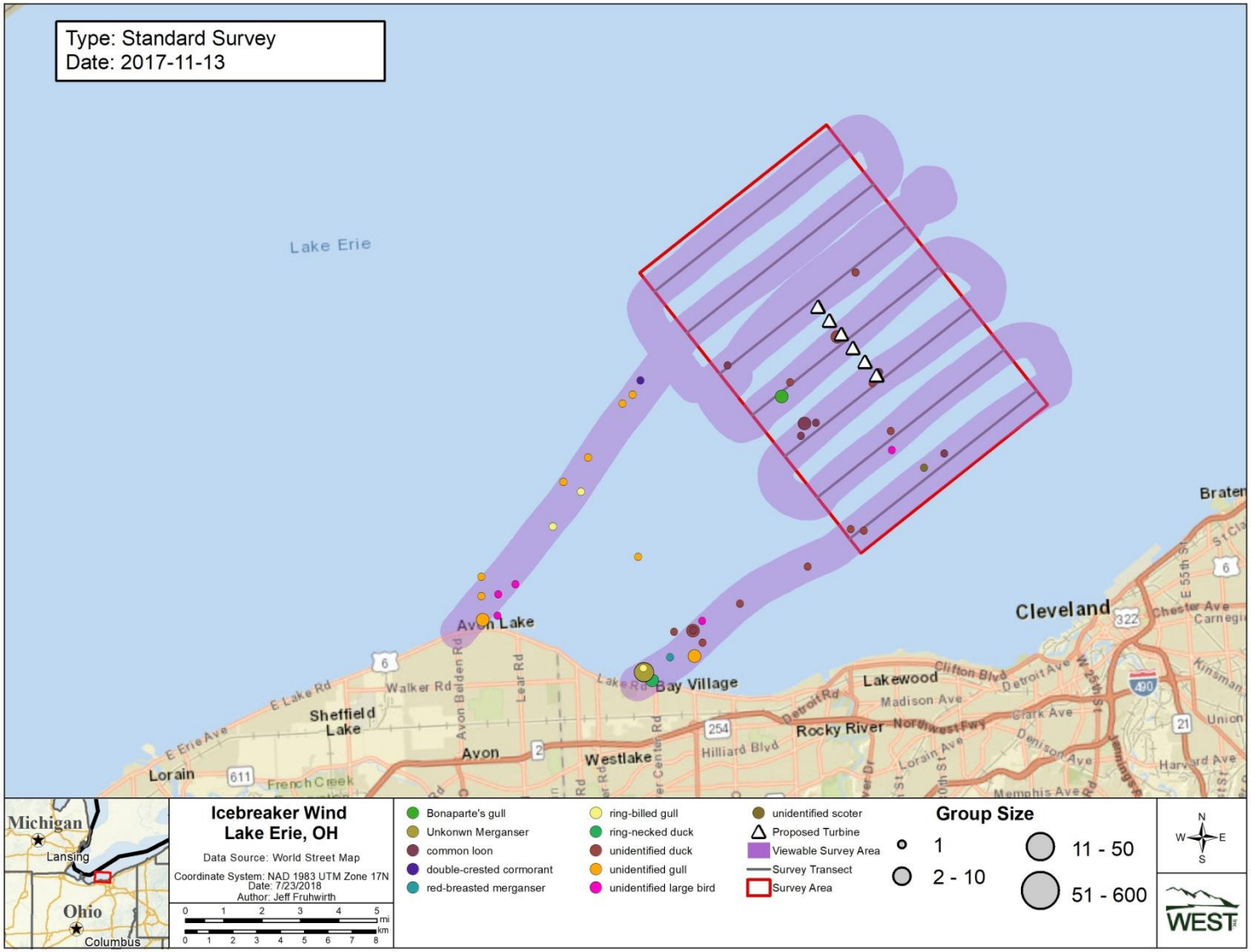

Appendix A-3. Location of the aerial survey area (red), 750-meter buffer survey track (purple), and number of birds (various colors; size of symbol indicates relative abundance) observed on November 13, 2017, for the Icebreaker Wind project. Bird counts and locations based on reconciled observation.

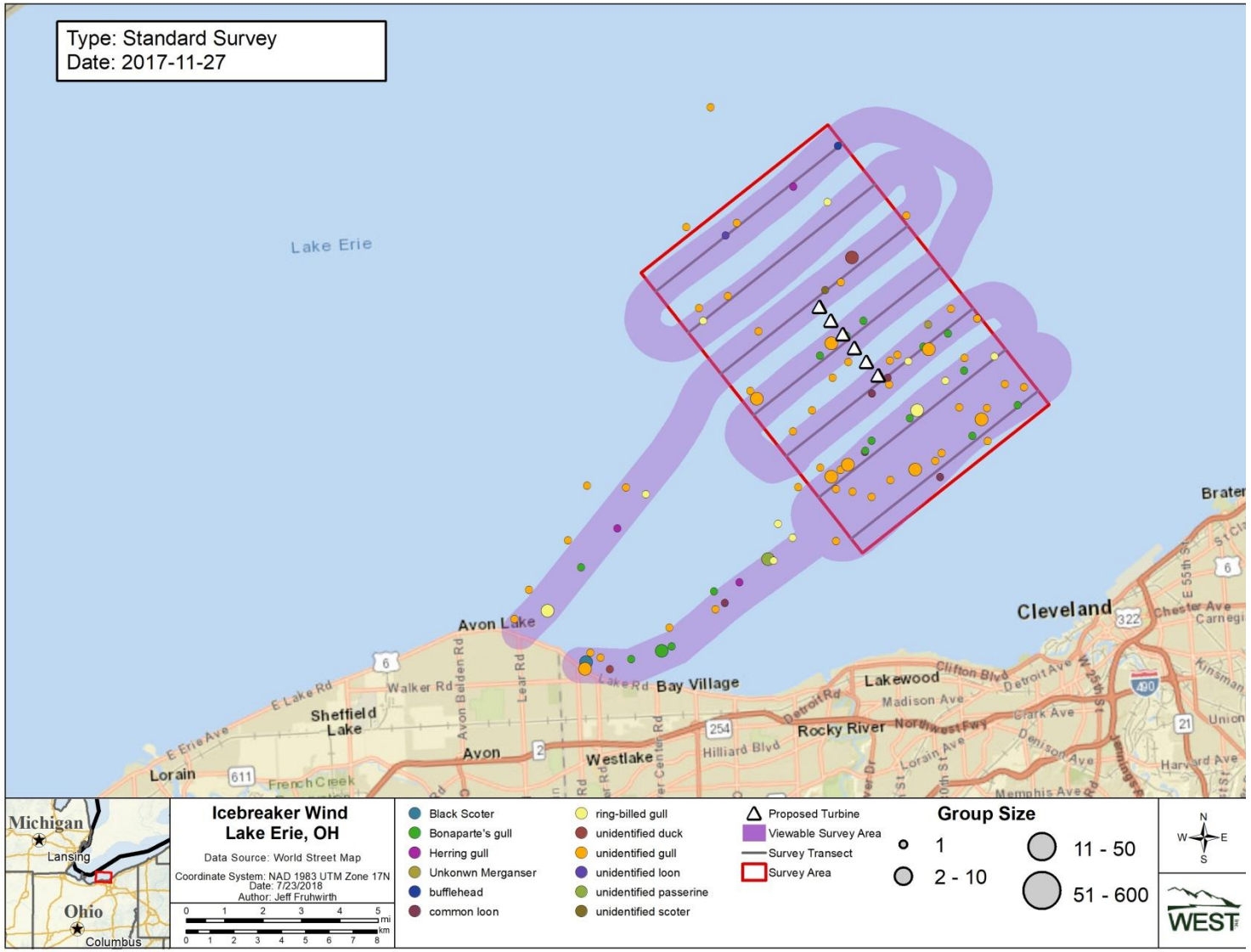

Appendix A-4 Location of the aerial survey area (red), 750-meter buffer survey track (purple), and number of birds (various colors; size of symbol indicates relative abundance) observed on November 27, 2017, for the Icebreaker Wind project. Bird counts and locations based on reconciled observation.

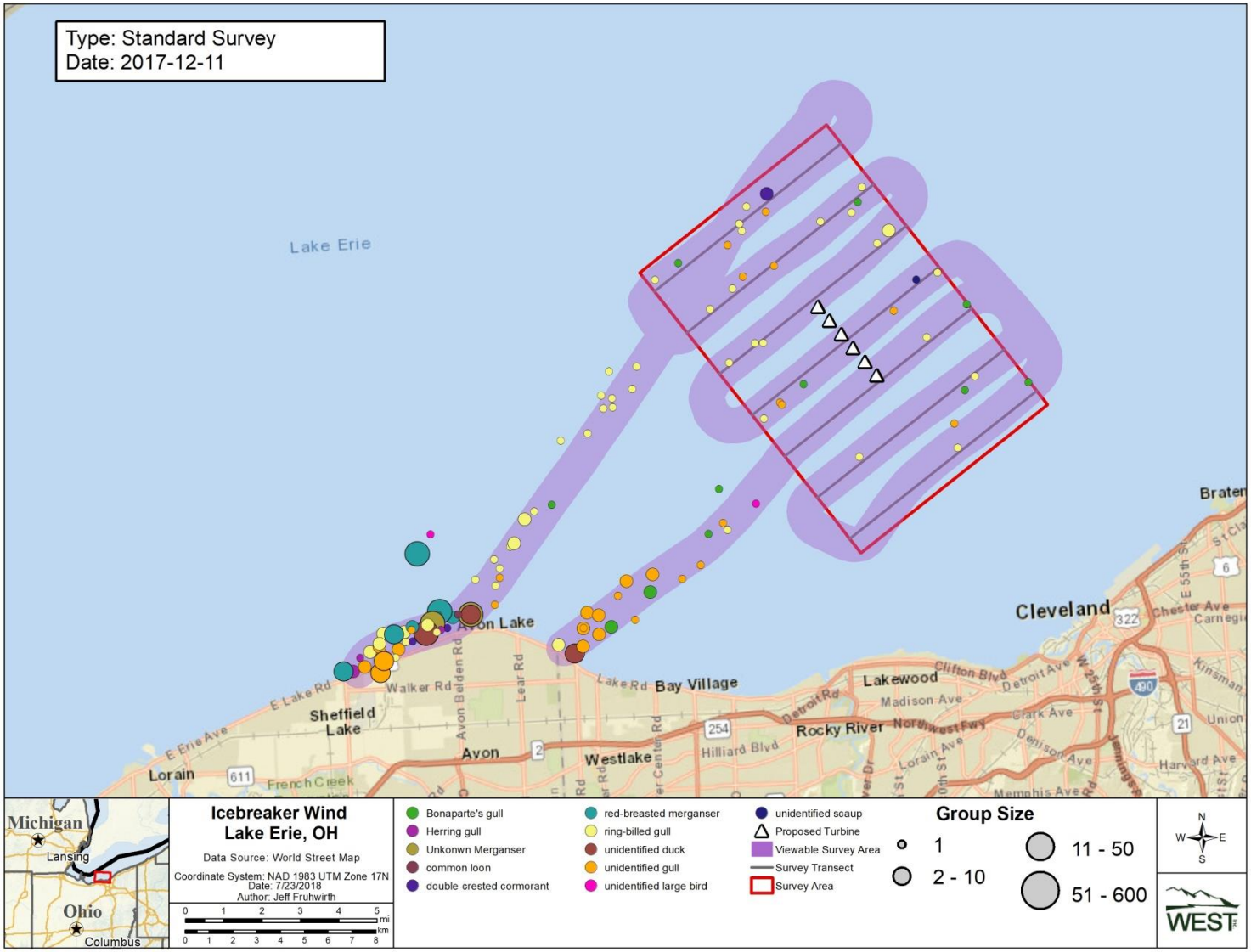

Appendix A-5. Location of the aerial survey area (red), 750-meter buffer survey track (purple), and number of birds (various colors; size of symbol indicates relative abundance) observed on December 11, 2017, for the Icebreaker Wind project. Bird counts and locations based on reconciled observation.

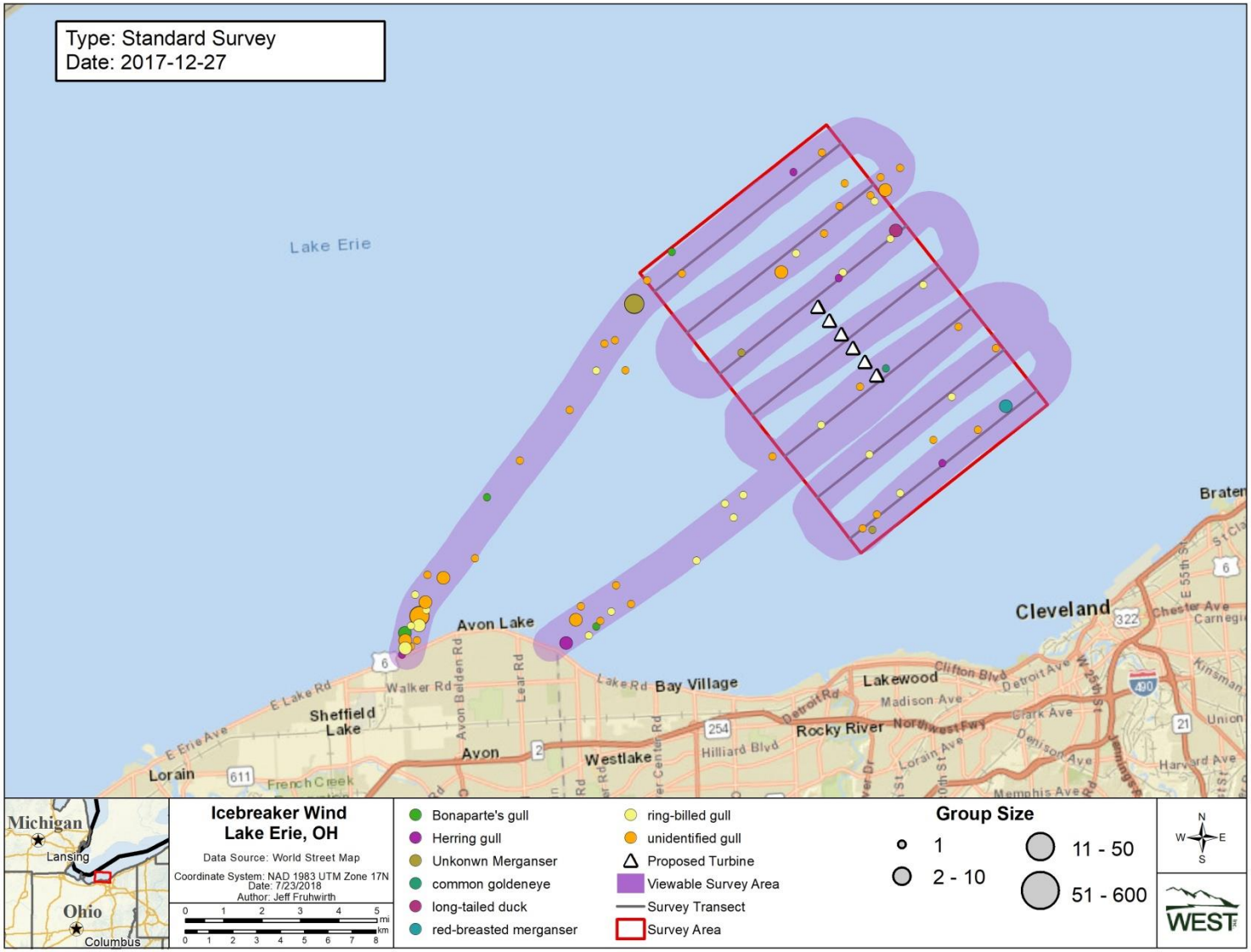

Appendix A-6. Location of the aerial survey area (red), 750-meter buffer survey track (purple), and number of birds (various colors; size of indicates relative abundance) observed on December 27, 2017, for the Icebreaker Wind project. Bird counts and locations based on reconciled observation.

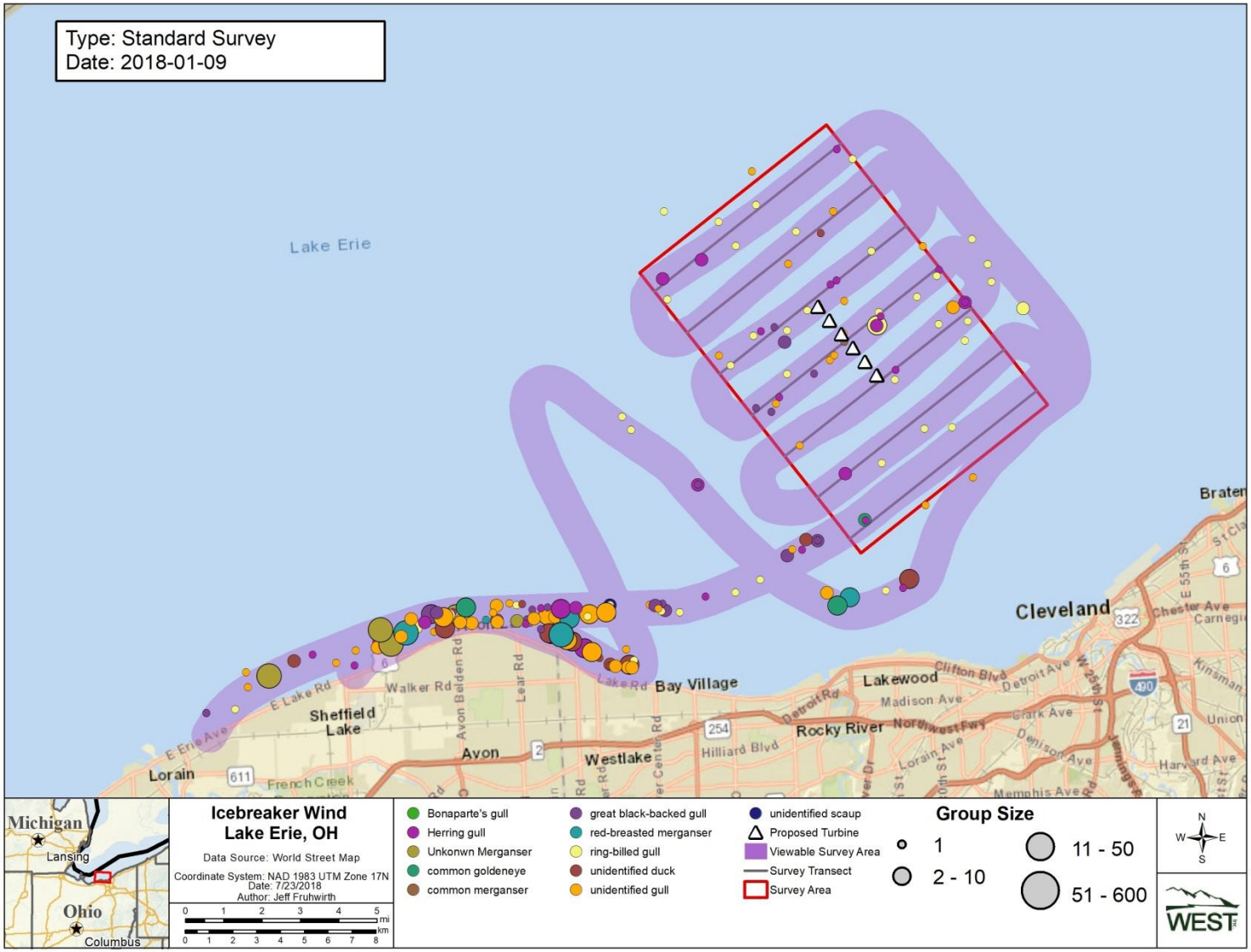

Appendix A-7. Location of the aerial survey area (red), 750-meter buffer survey track (purple), and number of birds (various colors; size of symbol indicates relative abundance) observed on January 9, 2018, for the Icebreaker Wind project. Bird counts and locations based on reconciled observation.

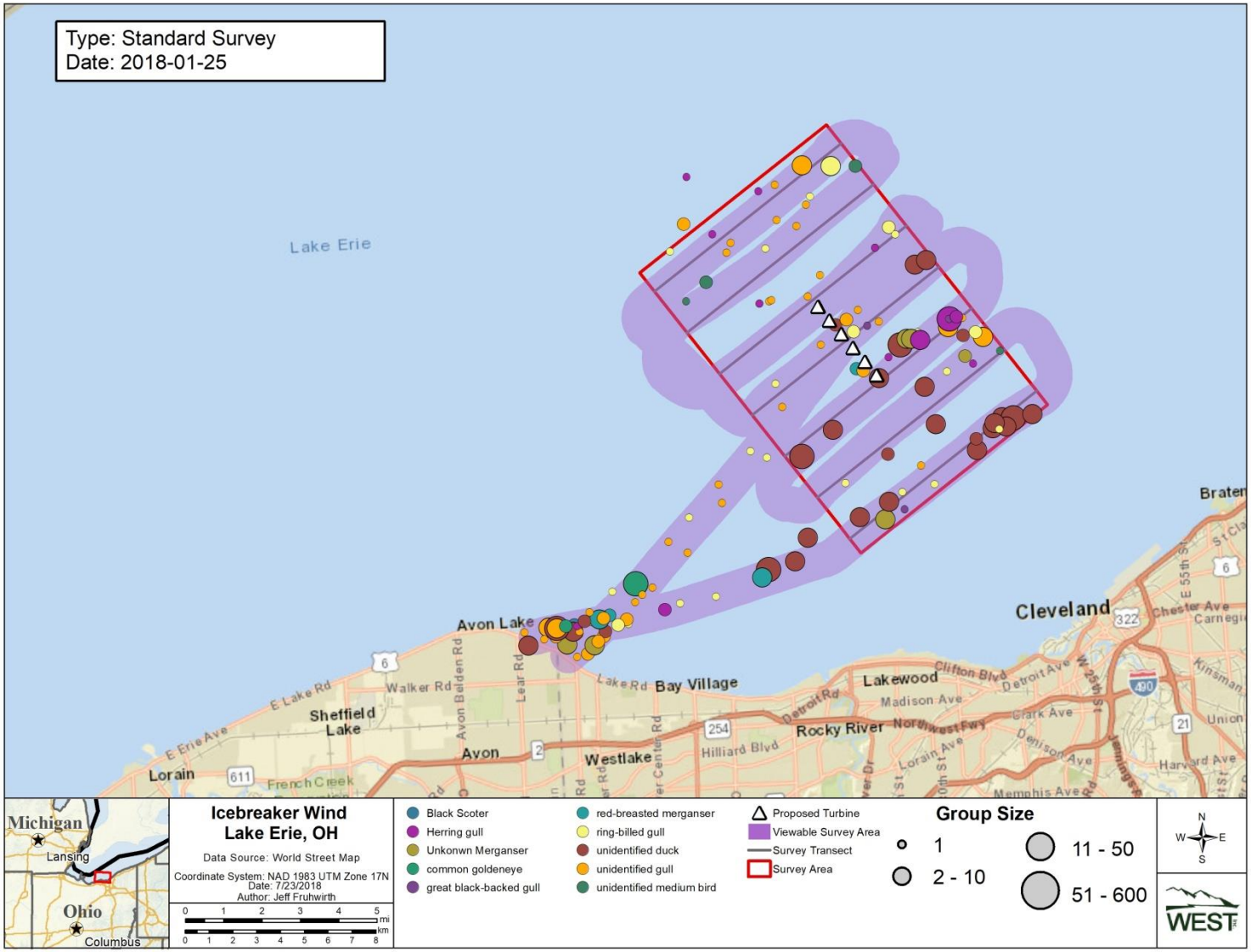

Appendix A-8 Location of the aerial survey area (red), 750-meter buffer survey track (purple), and number of birds (various colors; size of symbol indicates relative abundance) observed on January 25, 2018, for the Icebreaker Wind project. Bird counts and locations based on reconciled observation.

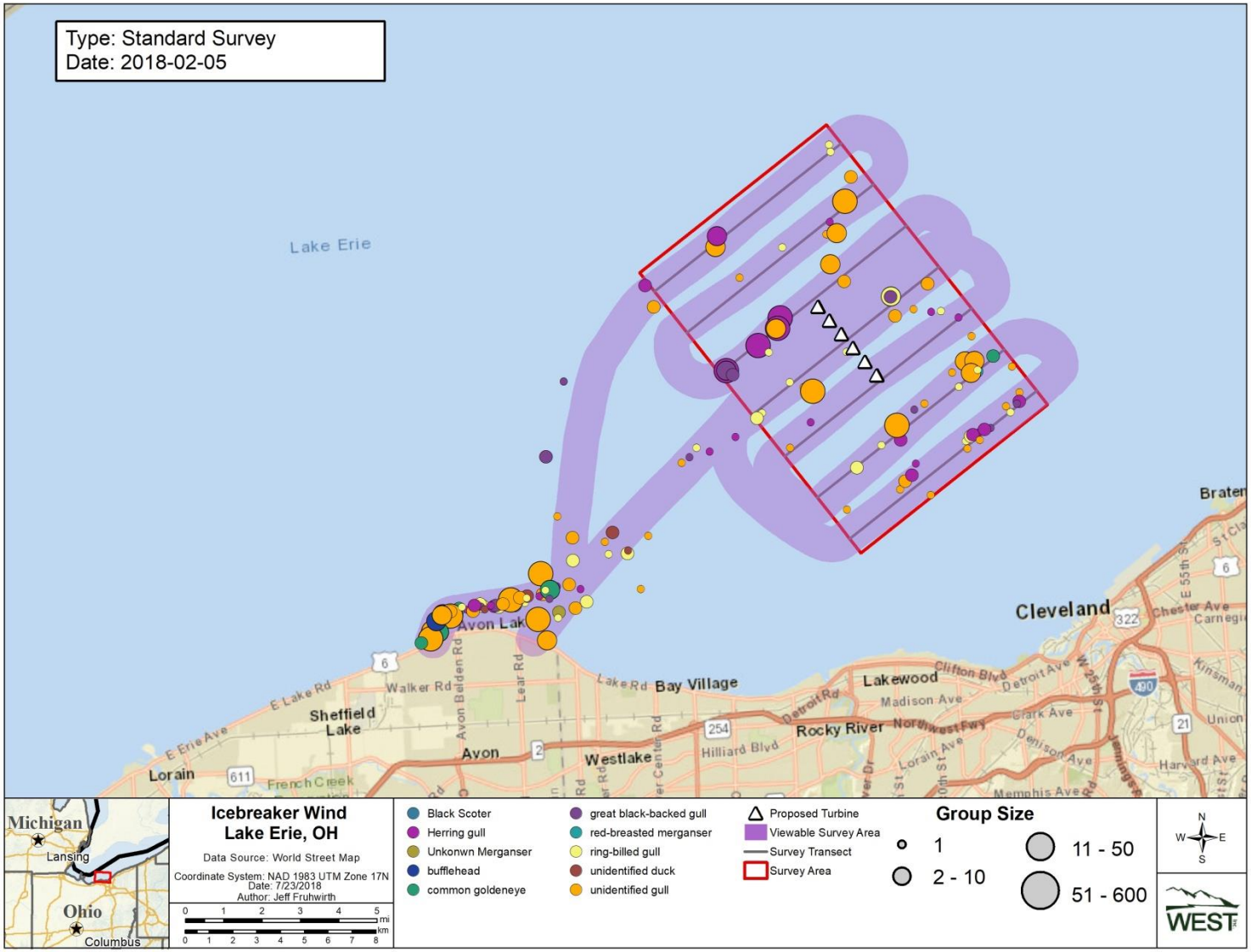

Appendix A-9. Location of the aerial survey area (red 750-meter buffer survey track (purple), and number of birds (various colors; size of symbol indicates relative abundance) observed on February 5, 2018, for the Icebreaker Wind project. Bird counts and locations based on reconciled observation.

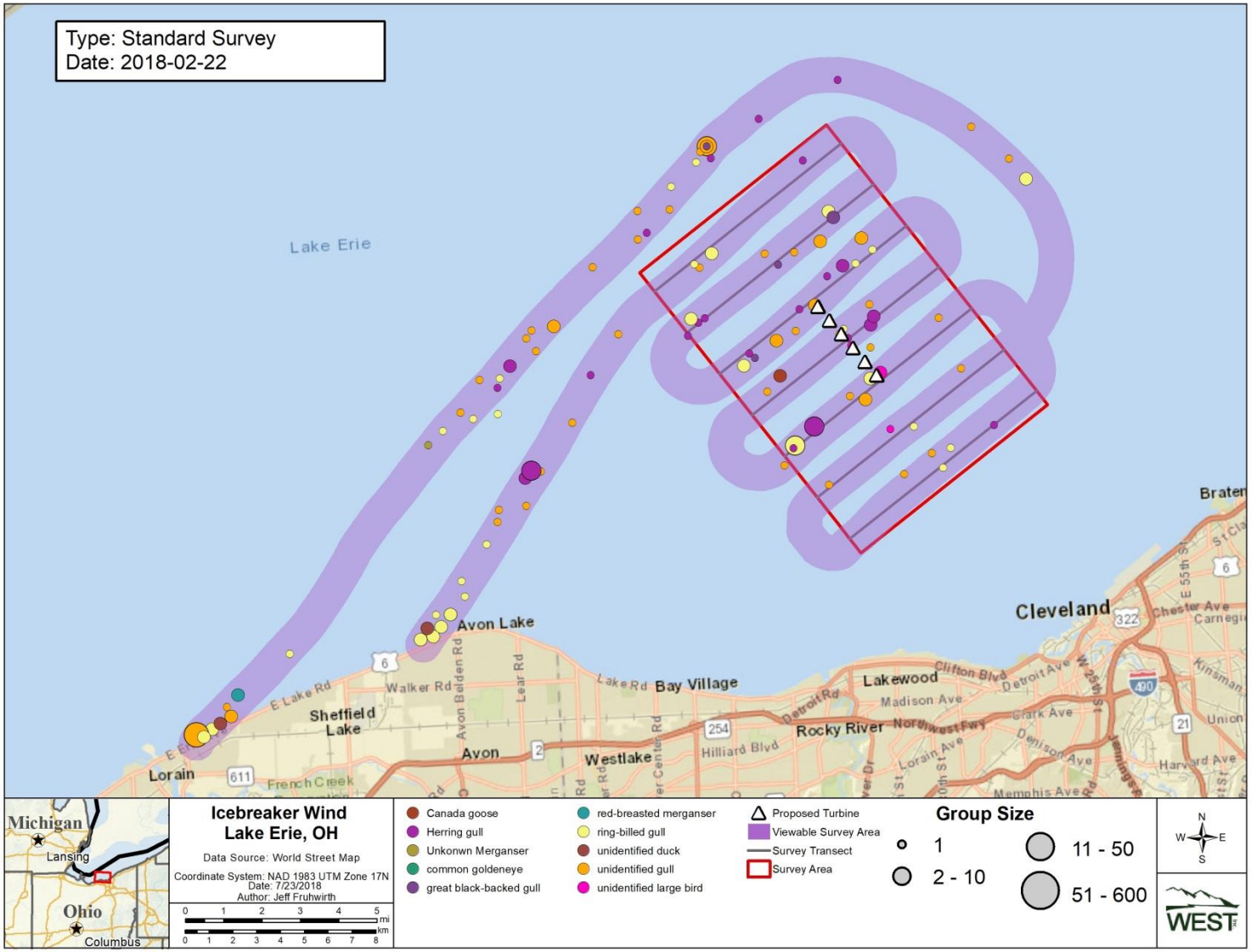

Appendix A-10. Location of the aerial survey area (red), 750-meter buffer survey track (purple), and number of birds (various colors; size of symbol indicates relative abundance) observed on February 22, 2018, for the Icebreaker Wind project. Bird counts and locations based on reconciled observation.

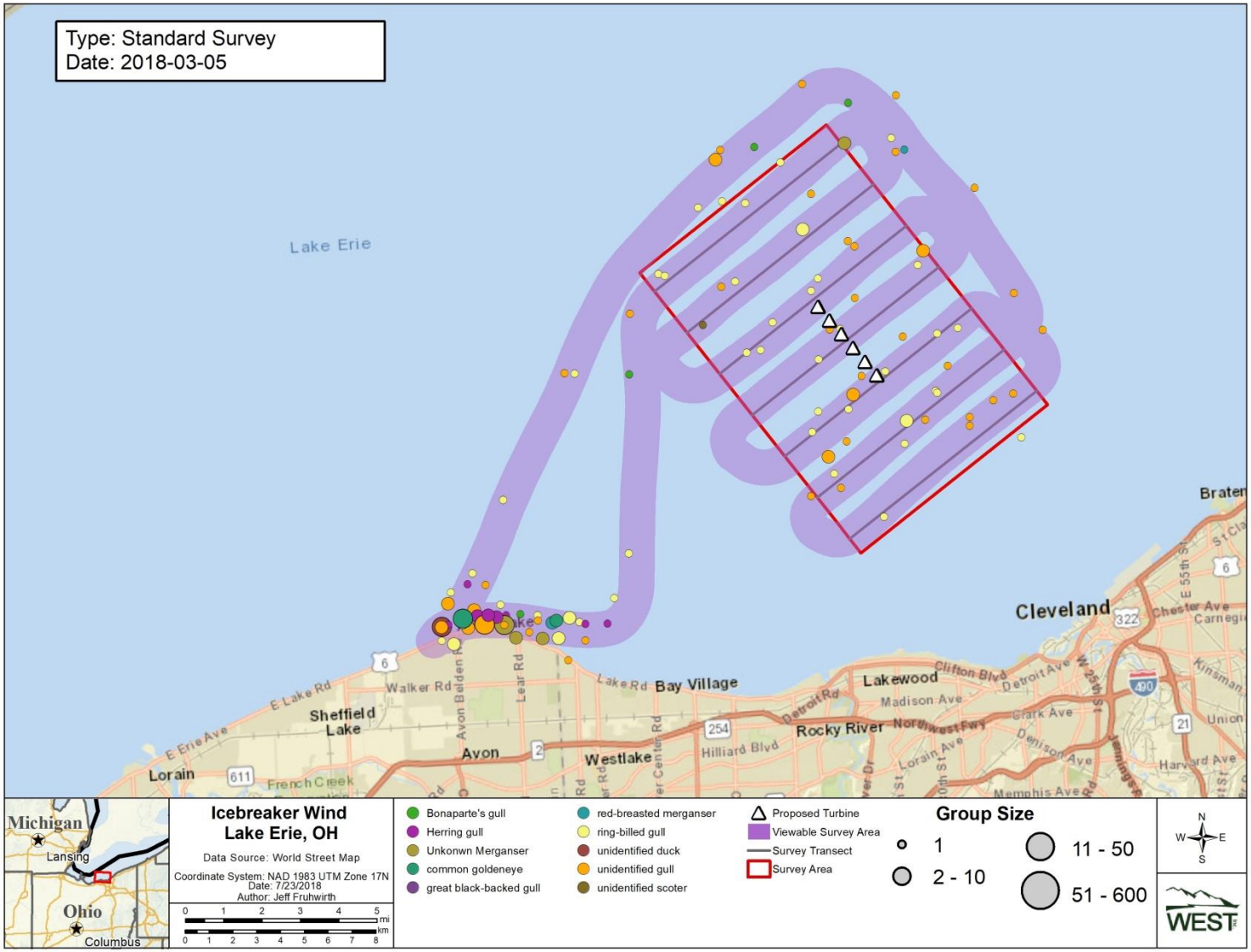

Appendix A-11. Location of the aerial survey area (red), 750-meter buffer survey track (purple), and number of birds (various colors; size of symbol indicates relative abundance) observed on March 5, 2018, for the Icebreaker Wind project. Bird counts and locations based on reconciled observation.

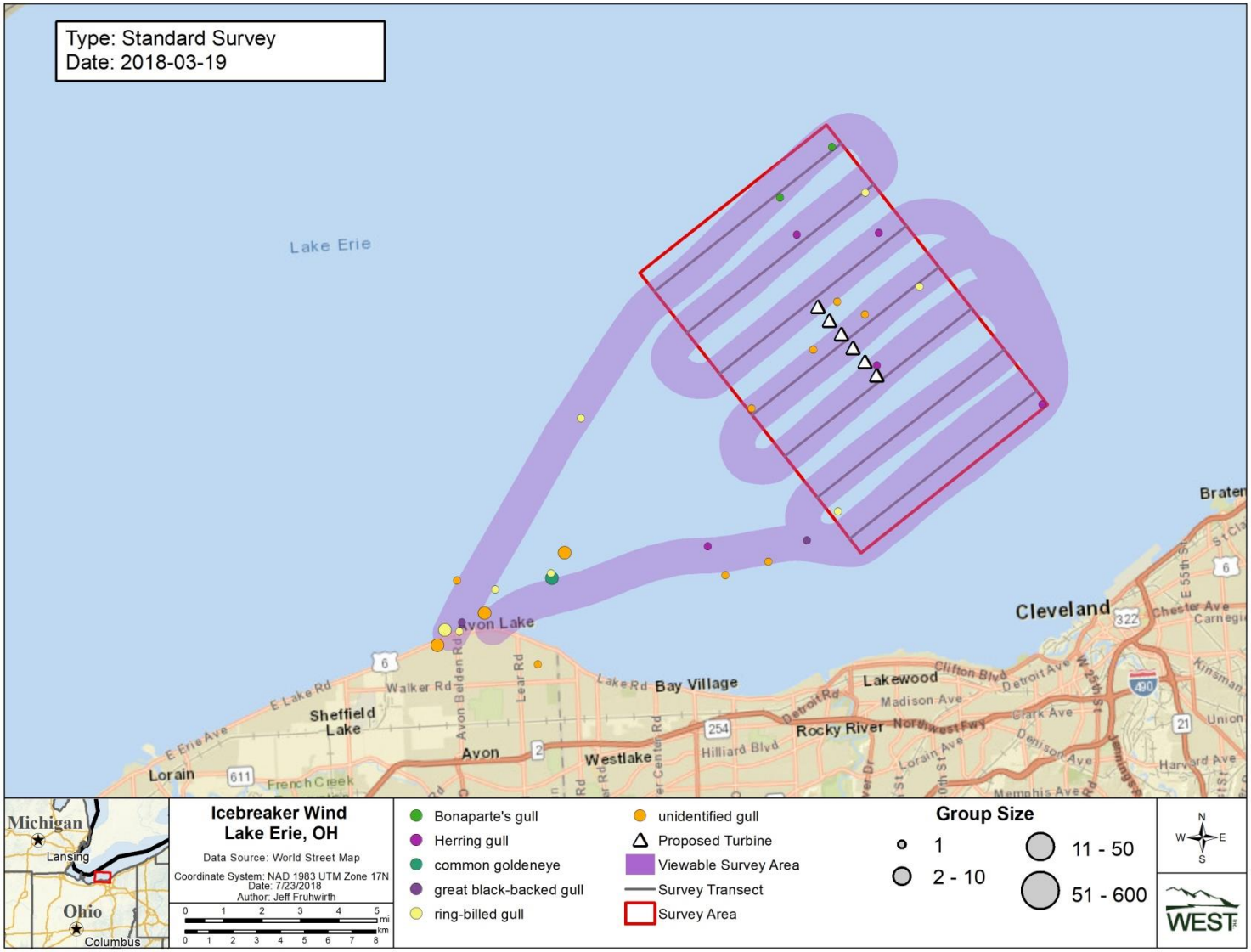

Appendix A-12. Location of the aerial survey area (red), 750-meter buffer survey track (purple), and number of birds (various colors; size of symbol indicates relative abundance) observed on March 19, 2018, for the Icebreaker Wind project. Bird counts and locations based on reconciled observation.

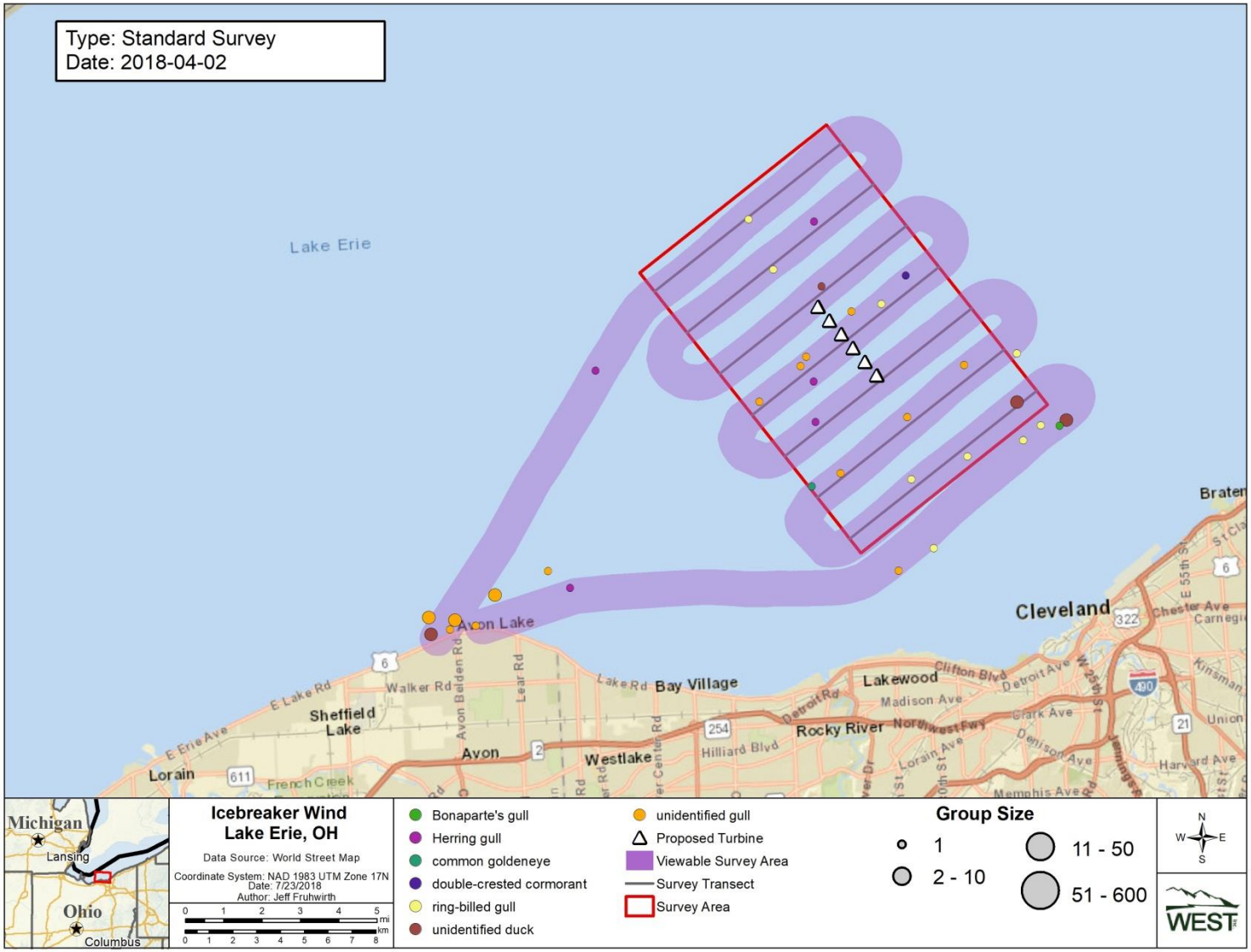

Appendix A-13. Location of the aerial survey area (red), 750-meter buffer survey track (purple), and number of birds (various colors; size of symbol indicates relative abundance) observed on April 2, 2018, for the Icebreaker Wind project. Bird counts and locations based on reconciled observation.

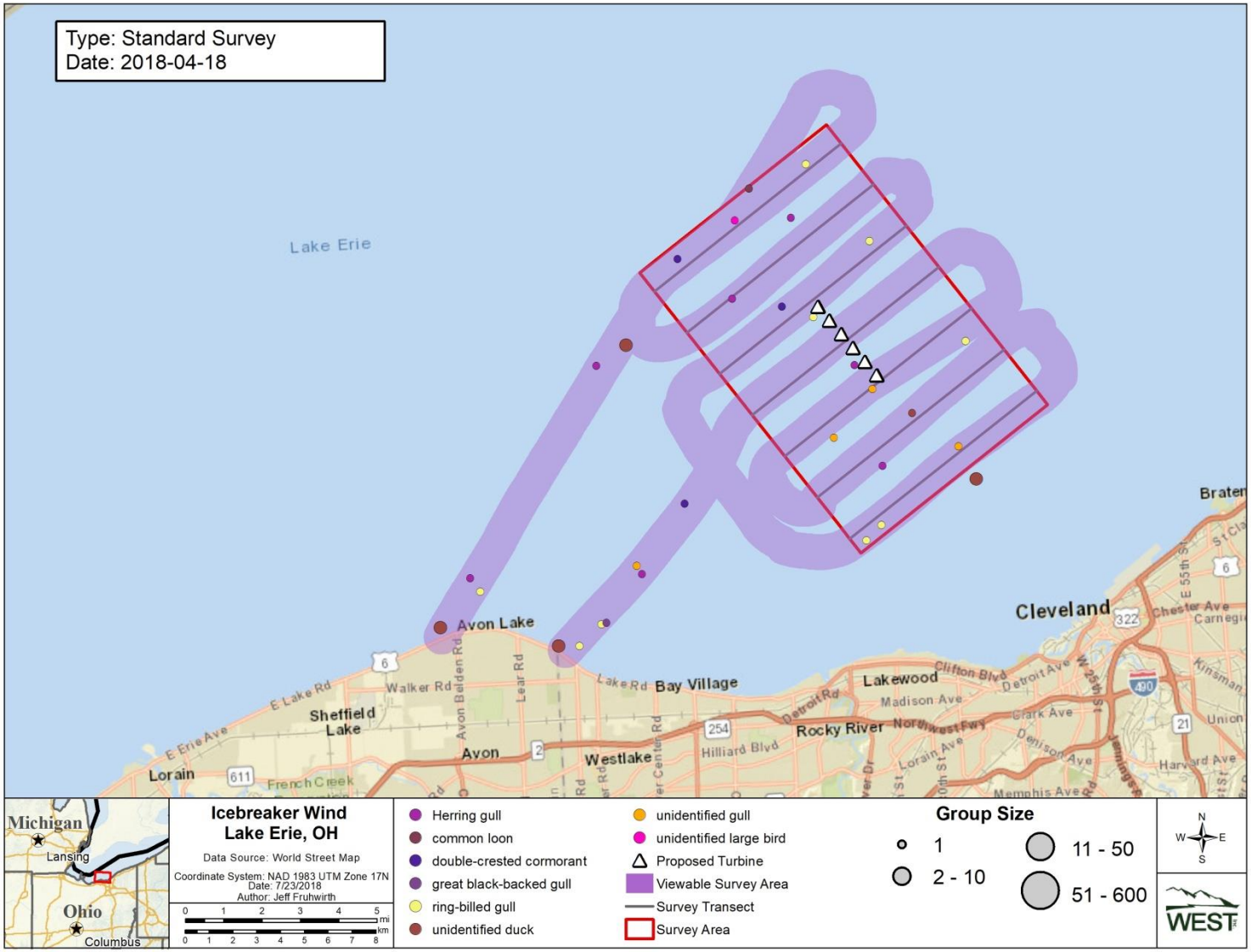

Appendix A-14. Location of the aerial survey area (red), 750-meter buffer survey track (purple), and number of birds (various colors; size of symbol indicates relative abundance) observed on April 18, 2018, for the Icebreaker Wind project. Bird counts and locations based on reconciled observation.

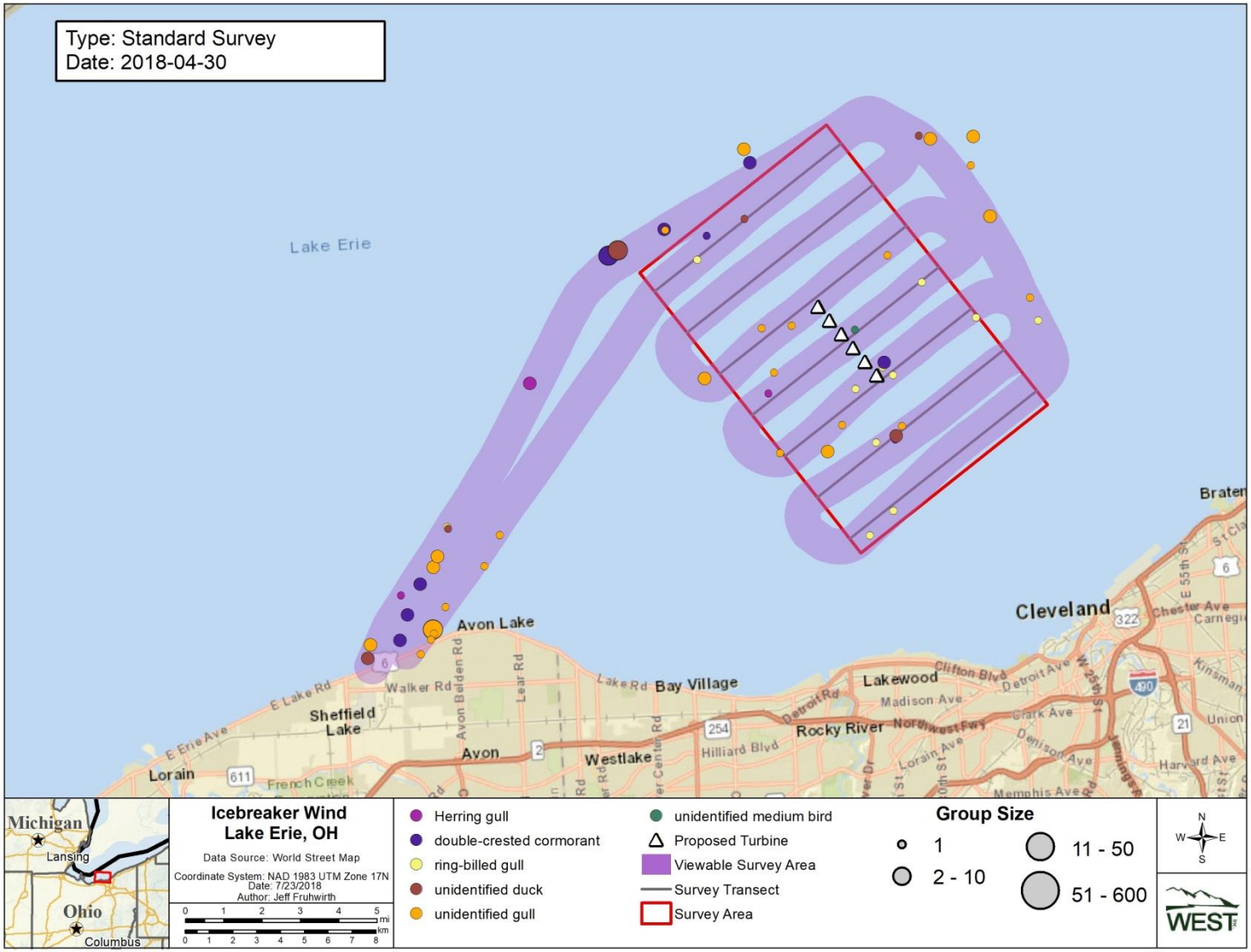

Appendix A-15. Location of the aerial survey area (red), 750-meter buffer survey track (purple), and number of birds (various colors; size of symbol indicates relative abundance) observed on April 30, 2018, for the Icebreaker Wind project. Bird counts and locations based on reconciled observation.

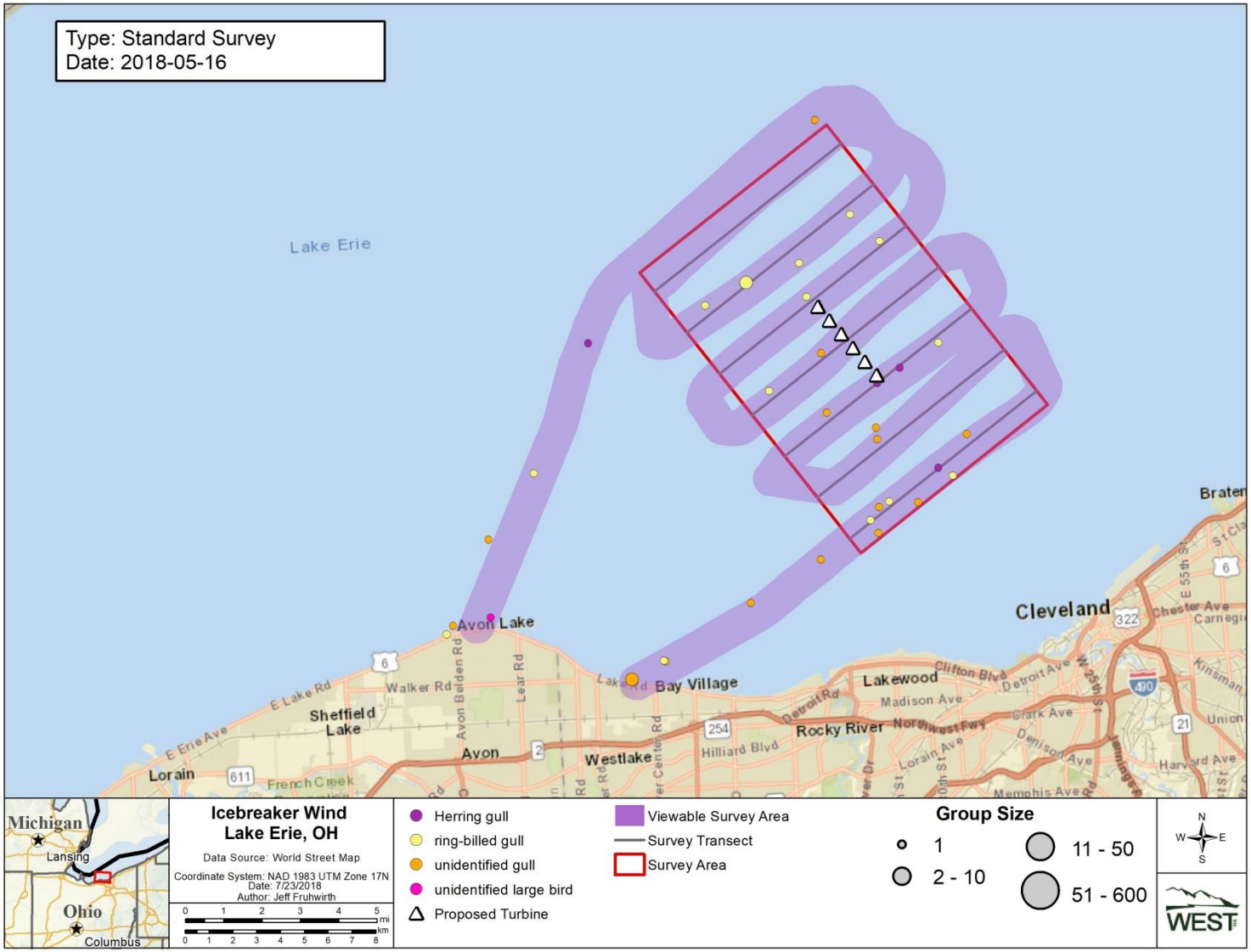

Appendix A-16. Location of the aerial survey area (red), 750-meter buffer survey track (purple), and number of birds (various colors; size of symbol indicates relative abundance) observed on May 16, 2018, for the Icebreaker Wind project. Bird counts and locations based on reconciled observation.

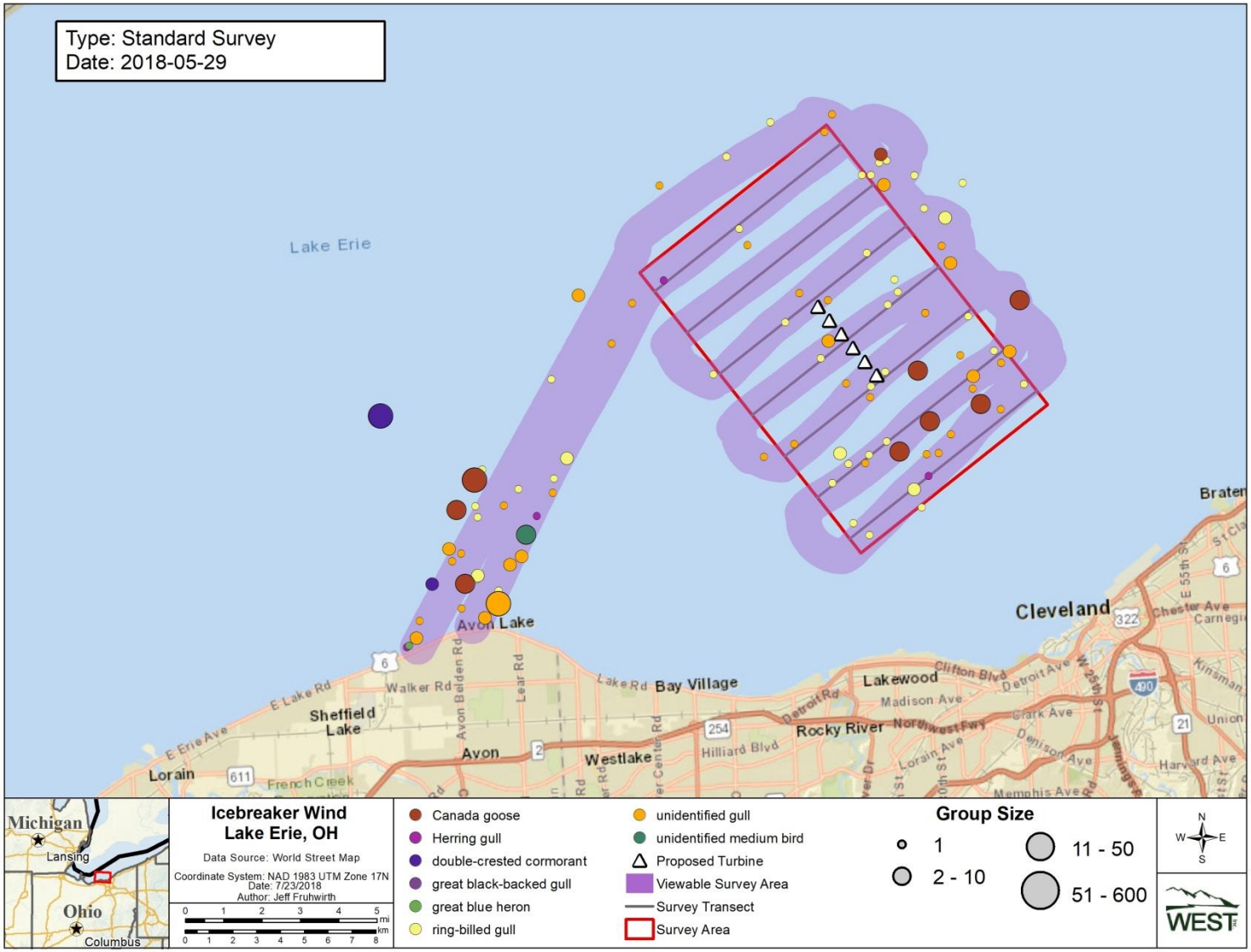

Appendix A-17. Location of the aerial survey area (red), 750-meter buffer survey track (purple), and number of birds (various colors; size of symbol indicates relative abundance) observed on May 29, 2018, for the Icebreaker Wind project. Bird counts and locations based on reconciled observation.

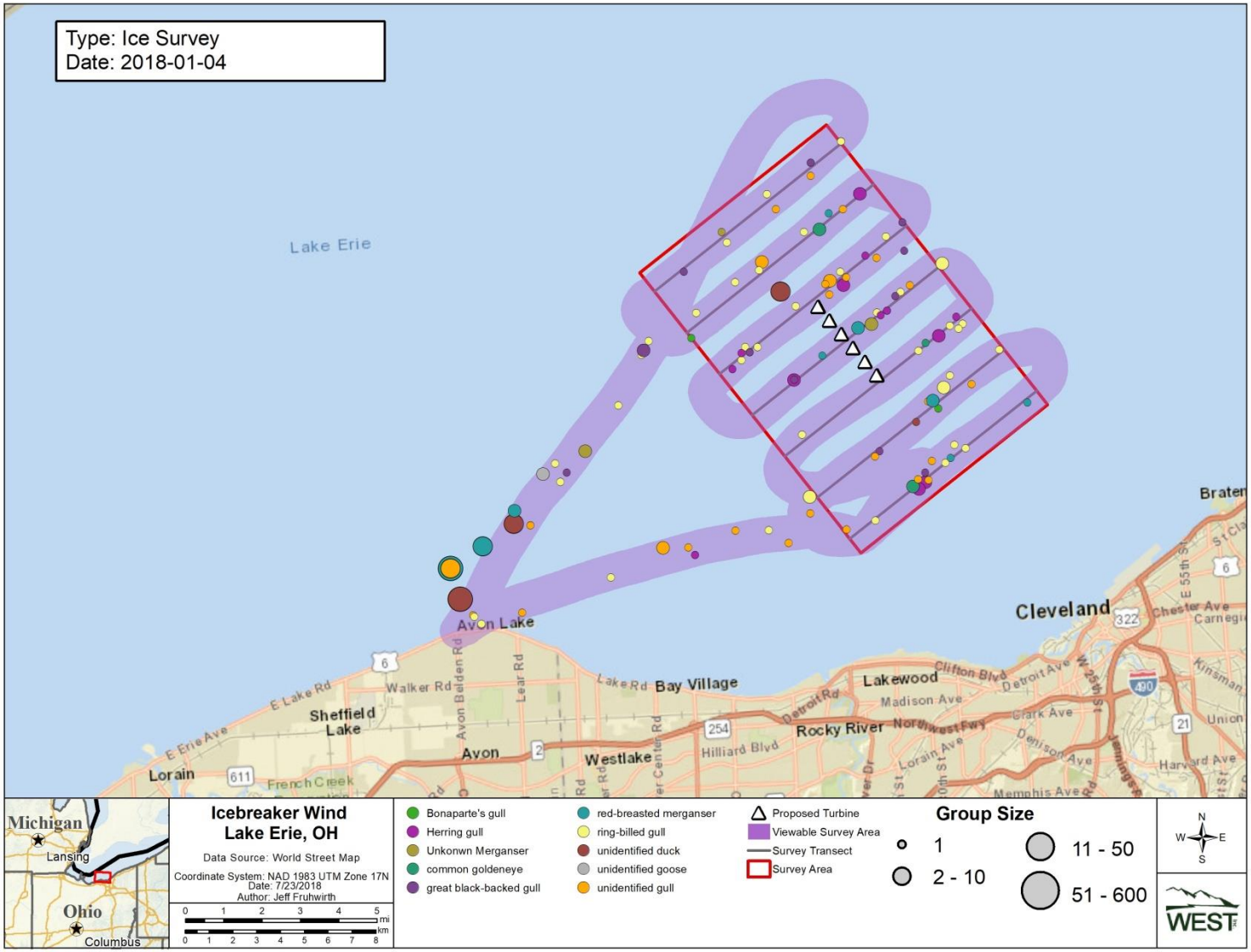

Appendix A-18. Location of the aerial survey area (red), 750-meter buffer survey track (purple), and number of birds (various colors; size of symbol indicates relative abundance) observed on January 4, 2018, for the Icebreaker Wind project. Bird counts and locations based on reconciled observation.

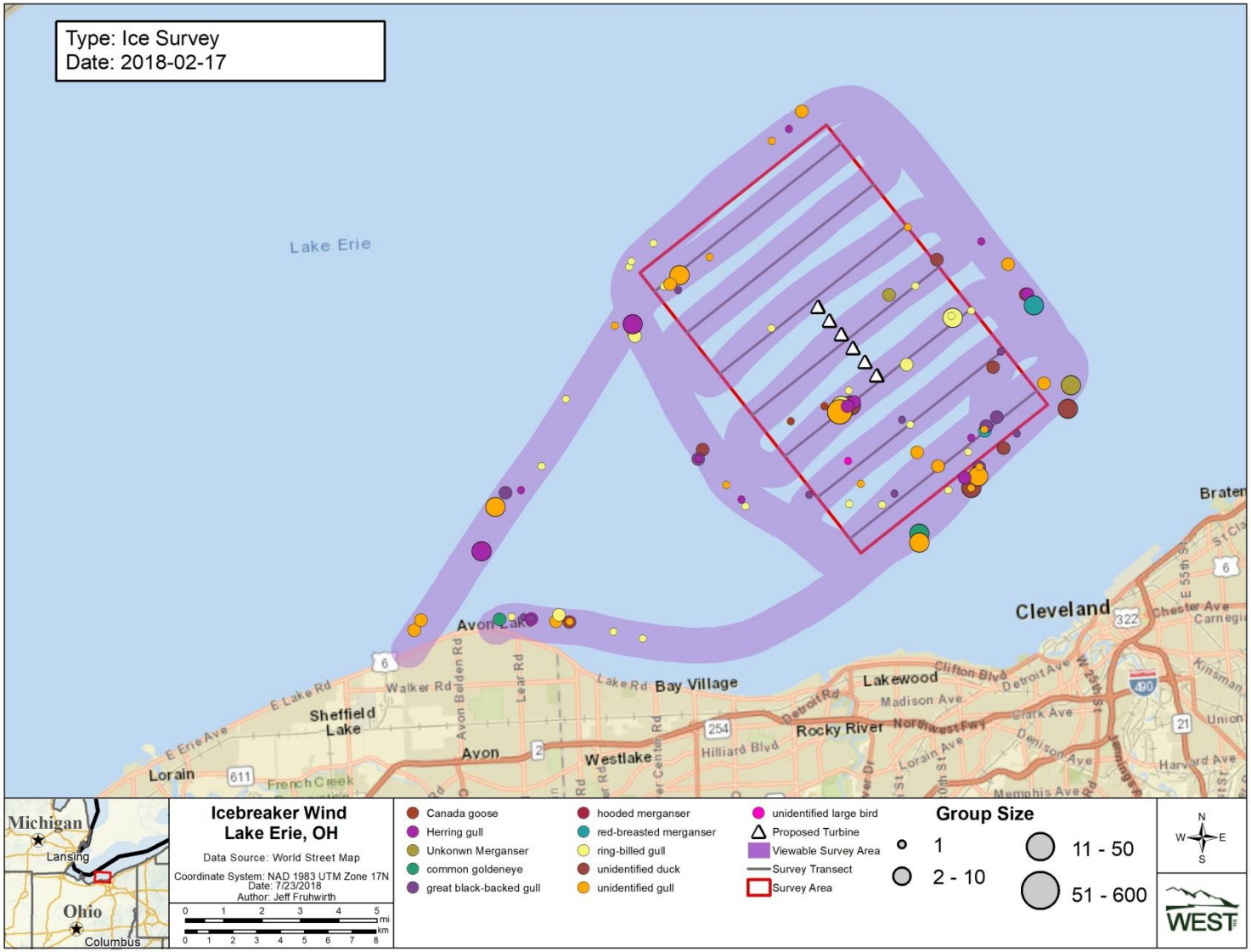

Appendix A-19. Location of the aerial survey area (red), 750-meter buffer survey track (purple), and number of birds (various colors; size of symbol indicates relative abundance) observed on February 17, 2018, for the Icebreaker Wind project. Bird counts and locations based on reconciled observation.